Investigation into the Effects of Real-world Uncertainties on A Computer Model-based Leak Detection System for Liquid Pipelines

by

Zhe Lu

A thesis submitted in partial fulfillment of the requirements for the degree of

Master of Science

in

Water Resources Engineering

Department of Civil and Environmental Engineering

University of Alberta

Abstract

Leaks in oil pipeline systems can significantly affect the environment and lead to economic losses. Pipeline companies are working to improve existing methods to monitor their pipelines more effectively. Computer model-based leak detection methods detect leaks by analyzing the pipeline hydraulic state and have been commonly employed in the energy pipeline industry. However, the effectiveness of these types of leak detection systems is often challenged by real-world uncertainties. This study quantitatively evaluated the impacts of uncertainties on leak detectability of a widely used real-time transient model based leak detection system. Uncertainties in fluid properties, data acquisition systems, and field sensors were assessed. Errors were introduced into the identified uncertainty sources one at a time and then randomly; and the changes in leak detection time caused by the real-world uncertainties were quantified using simulated leaks. This study provides valuable quantitative results contributing towards a better understanding of how real-world uncertainties may affect leak detection. A general ranking of the importance of the uncertainty sources was obtained; ordered from high to low, they are time skew, bulk modulus error, viscosity error, and polling time. It was also shown that inertia-dominated systems with low R factors were less sensitive to uncertainties compared to friction-dominated systems with high R factors.

Acknowledgements

The author would like to express the greatest gratitude to his supervisor, Dr. Yuntong She, for her kind guidance and assistance in all aspects of this project. All the patient help is very much appreciated. Thank you as well to Dr. Huazhou (Andy) Li and Dr. Evan Davies for being in the oral examining committee.

This research is supported by Enbridge Pipelines Inc. and by the National Sciences and Engineering Research Council of Canada Collaborative Research Development, which are gratefully acknowledged.

The author would also like to thank his parents for their endless love and support, and his friends for their warm encouragement through the Master program.

Table of Contents

List of Tables

List of Figures

Chapter 1: Introduction

1.1 Background

Pipelines are considered a reliable, efficient, and environmentally-friendly way of delivering large quantities of crude oil over long distances. The World Factbook (Central Intelligence Agency – CIA, 2016) indicates that the pipelines span approximately 119,000 km across Canada. The networks of pipelines in Canada are vast with approximately 1.2 billion barrels of oil products transported every year and contributed $11.5 billion to the national gross domestic product (GDP) in 2015 (Canadian Energy Pipeline Association – CEPA, 2016).

The safety of pipelines is one of the top priorities for the pipeline industry. Pipeline companies have been taking various measures to maintain and monitor their pipelines. Extensive federal and provincial regulations are in place but the existence of pipeline leaks cannot be eliminated. Many factors may lead to pipeline leak, such as metal loss, cracking and fatigue of pipelines. The National Energy Board (NEB) indicates that during the period of 2008 to 2016, a total of 59 liquid release events have been reported, which caused volumetric loss of crude oil summing up to 1,765.38 m^3. Leaks not only pollute the land and resources of the affected areas significantly, but also cause significant economic losses, including costs of a timely contaminants cleanup, thorough incident investigations, and pipeline repairs. For instance, a severe crude oil leak accident that took place in Michigan, United States, in 2010 released more than 8,000 barrels of liquid products into Talmadge Creek and Kalamazoo River, and a total of approximately $785 million was spent on pollutant cleanup (Enbridge Inc.). Therefore, detecting leaks is

an ongoing challenge and the pipeline industry is highly motivated to enhance the current leak detection technologies and develop new ones.

The energy pipeline industry is employing highly sophisticated technologies and practices for leak detection. Some of these techniques are based on devices installed externally to the pipeline systems. For example, wireless digital sensors may be attached around a pipeline to sense the signal of leaking fluid products (e.g. pressure drop), and other sensors may be installed in the soil around the pipelines to detect the presence of hydrocarbons (CEPA, 2016). These technologies are limited to high-risk regions due to high installation and maintenance costs and the associated retrofit challenges for existing pipelines (Geiger, 2006). Other techniques use field measurements of internal pipeline parameters and produce new values via some kind of algorithmic computation. If the calculated new values exceed certain thresholds, an alarm is generated that may indicate a leak (American Petroleum Institute - API, 2002). This type of method is called computational pipeline monitoring, which has the advantage of being relatively non-invasive (to the pipe) and requiring no field installation.

The algorithm adapted in the computational pipeline monitoring method can be as simple as a mass balance calculation, or as sophisticated as a full-blown hydraulic transient model, i.e. *real-time transient model* based leak detection method. The occurrence of a leak creates a transient event, i.e. pressure waves propagating in both directions along the pipeline. Therefore, analyzing hydraulic behaviors (particularly pressure and flow rate) makes it possible to detect leaks. A computer model is perfect for this purpose. By solving the partial differential equations of conservation of mass, momentum, and energy given necessary pipeline characteristics and boundary conditions,

the hydraulic state along the pipeline can be computed in real time. The other main component of a *real-time transient model* based leak detection method is a supervisory control and data acquisition (SCADA) system. The SCADA system obtains the measured data from field sensors and writes the data into a Remote Terminal Unit (RTU) data file. A leak is suspected when the model computed pipeline state (primarily pressure and flow) deviates from the corresponding field measurement data in the RTU data file. An alarm will be generated when the discrepancies exceed certain threshold(s). A *Real-time transient model* based method is the core technology of many commercial leak detection software programs such as DNV-GL *Synergi Pipeline Simulator (SPS) Statefinder* and is the focus of this study.

1.2 Problem Statement

The effectiveness of *real-time transient model* based leak detection methods in practical applications is often challenged by real-world uncertainties. The pipeline characteristics (e.g. pipe diameter, length, wall thickness, and elevation profile) and fluid properties (e.g. density, viscosity, and bulk modulus) may not be known accurately. Field sensor measurements can be inaccurate or contain data noise. The SCADA system polls data from field sensors at discrete time and therefore between the polling intervals (polling time) there is uncertainty. In addition, the SCADA system polls data from each sensor consecutively rather than from all field sensors simultaneously. Sensors at different locations are polled at different time but stamped at the same time, causing a "time skew". These uncertainties contribute to discrepancies between the model predicted pipeline state and that as indicated by the measured data even when no leak is present.

Detection of small leaks often needs relatively tight alarm threshold values. However, the magnitude of discrepancies caused by real-world uncertainties may be close to or even bigger than those caused by a small leak (USDOT, 2007). False alarms are often resulted (giving an alarm when no leak is present). Too many false alarms reduce the reliability of the leak detection system, and can potentially lead to missing the alarms caused by a real leak. A relaxed alarm threshold can reduce the number of false alarms, but will cause small leaks become undetectable. This problem can be bigger when pipeline is operating under transient conditions, e.g. during the pump and valve operations, pipeline start-up and shut-down. It has been observed that leak detectability degrades during transient operating conditions (personal communication Enbridge Pipelines, 2013). Transient operating conditions can be quite frequent in pipeline systems. The possibility of a leak occurring during transient conditions is not lower than during steady sate. Therefore, it is important to evaluate the effects of uncertainties on leak detectability during various operating conditions (both steady state and transient state).

1.3 Previous Research

Many studies have been conducted to investigate the impact of uncertainties on hydraulic modelling and leak detection of water distribution systems. Some focused on steady state. For example, Al-Zahrani and Muhammad (2014) assessed the effects of uncertainties of pipe roughness and initial tank level on the modelled pressure heads at pipe junctions. A *Monte-Carlo Simulation (MCS)* method was used to generate random values for pipe roughness coefficient and water tank level. These values were input to the hydraulic model *EPANET* which solves the continuity and the conservation of energy

equations iteratively for water distribution systems (Rossman, 2002). The results indicated that modelled pressure was less sensitive to uncertainty in pipe roughness than uncertainty in the tank level.

Others focused on transient conditions. Covas and Ramos (2010) assessed the effectiveness of *Inverse Transient Analysis (ITA)* leak detection method using the pressure and flow rate data collected with different leak sizes from two experimental facilities and one real-world water transmission system. *ITA* integrates a hydraulic transient model with an optimization algorithm. Leak sizes were determined through optimization which minimizes the difference between observed and calculated pressure values; leak locations were determined based on the travelling time of transient signal from the source to the leak. Transient events in laboratory were generated by operating a valve at the downstream end of the pipe. In field conditions, the transient was generated by shutting down the upstream valve while keeping the downstream valve open during data collection. The *ITA* method was shown to be able to detect and localize leaks of reasonable sizes (10% of line rate or larger). It was found that the modelled wave speed was lower than that calculated based on pressure signal travelling time. The difference between the actual and estimated wave speed was attributed to the uncertainties in physical characteristics (e.g. diameter changes and non-elastic behavior of pipe), which significantly affected the leak detectability. The uncertainty in data collection also contributed to the degraded leak detectability since the sensor accuracy and noise greatly affected the identification of the leak pressure drop.

Duan (2015) examined the effects of uncertainties on leak detection during transient condition. The investigation was conducted with a water hammer model, which

solves the conservation of mass and momentum equation neglecting the convective terms. Leak detection was achieved by using the frequency domain method which detected and localized leaks utilizing the leak-induced damping pattern of peak in the frequency domain (Duan et al. 2011). A hypothetical water distribution system was established with constant diameter, constant tank level at upstream and downstream, and a valve at downstream end to adjust the pipe flow rate. Transients were generated by shutting down the downstream valve. Effects on leak detection by uncertainties in the initial Reynolds number, valve operation time, pressure measurements, and wave speed were evaluated both individually and collectively. The results showed that the uncertainties in wave speed and pressure data measurement had greater impacts on the leak detection method than those in valve operation time and initial Reynolds number.

The properties of water are very different from the properties of oil transported in energy pipeline systems. Studies on water distribution systems focused on junctions and branches while the energy pipelines are generally long single pipelines. Whether or not the findings of the water distribution system studies can be transferred to the energy pipelines needs further investigation. However, most research in energy pipeline field focused on the enhancements of model-based leak detection methods. For example, Al-Khomairi (2008) developed a new method of leak detection for long pipelines. Trial leaks were introduced into the simulated pipeline. The leak size and location were determined as the ones that minimize the squares of the discrepancies between computed and measured values of flow rate and pressure. This method was verified with water using lab experiments and was shown to be satisfactory in detecting small leaks (as small as 1% of line rate) during both steady state and transient state.

Research of the effect of uncertainty on leak detection systems in energy pipelines is relatively limited and American Petroleum Institute (API) 1149 appears to be the only applicable publication that discusses the effects of variable uncertainties on leak detection for energy pipeline systems (American Petroleum Institute, 1993). Initially published in 1993, API 1149 discussed the sources of uncertainty including pipeline systems characteristics, fluid properties, and data noise as well as their ranges. The leak detection system used to evaluate how uncertainties affect leak detection employed a water hammer model to simulate the pipeline state assuming the pipeline was intact. A "pattern recognition" algorithm was used for leak detection, i.e. a leak was declared when the differences between measured and calculated data matched a specific leak pattern (e.g. a simultaneous pressure drop at the inlet and a rise in the inlet flow rate; immediate drop in both pressure and flow rate at the outlet). A similitude parameter named *R* factor was developed to categorize the pipelines.

$$R = \left(\frac{V_0}{2a}\right)\left(\frac{Lf}{D}\right) \tag{1-1}$$

R factor consists of five variables including initial velocity (V_0), friction factor (f), wave speed (a), pipe length (L) and diameter (D). It was shown that pipelines with identical *R* factor values have the same hydraulic behaviors, which allowed the reduction of number of test scenarios and generalization of the test results. API 1149 (1993) indicated that the effect of uncertainty in each of the five variables comprising the *R* factor was identical to the effect of uncertainty introduced to the *R* factor. Therefore, the effect of uncertainty on leak detection can be evaluated by introducing the uncertainty to *R* factor alone rather than to each of the five variables individually. It was concluded that pipeline systems with low *R* factors were generally more tolerant to uncertainties as compared to those

with high *R* factors. As these findings were based on pattern recognition leak detection algorithm, their applicability to other prevailing leak detection algorithms needs further investigation.

API 1149 was updated in 2015 and provided a framework to assess the effect of uncertainties on a full range of computational pipeline monitoring methods currently in use (American Petroleum Institute, 2015). It described a general procedure as the following. A hydraulic model is built for a hypothetical pipeline to establish a reference pipeline state. The measurement and configuration data with introduced error are then used to run the computational pipeline monitoring system for various operating scenarios. With the uncertainties, the computational pipeline monitoring system will show some indications of leak when there is none. This produces statistical properties of the false indication of leak. A case study was conducted and the uncertainty associated with the SCADA system was included. It was shown that time skew had a significant impact on leak detectability during transient period, greater than the effect of pressure measurement error but smaller than the flow rate measurement error. However, the conclusions were made using a simple mass balance method in this case study thus may not be applicable to the more sophisticated *real-time transient model* based leak detection systems.

1.4 Objective

The objective of this research was to improve our understanding of the effects of real-world uncertainties on the performance of a widely used *real-time transient model* based leak detection method. This is important for pipeline companies to prioritize improvement measures when enhancing their leak detection system. The objective was

achieved by introducing uncertainties into leak detection system and quantifying the change in leak detectability under various operating scenarios. Simulated leaks were used to test the response of the leak detection system. The broadly applied *SPS Simulator* and *Statefinder* (DNV-GL) were selected to facilitate this study. *SPS Simulator* is used by over 130 companies worldwide and was used in this study to generate simulated leak data. *SPS Statefinder* is what Enbridge's leak detection systems of over 30 pipelines are built upon and is used by over 30 other companies. It consists of a *real-time transient model* and an optimization based leak detection algorithm. In this study, uncertainty was first introduced to each of the selected key variables (e.g. viscosity, bulk modulus, time skew, polling time, and measurement data) one at a time, and then errors were randomly generated for all five variables using *MCS* method. The effects of uncertainty on the low *R* and high *R* systems were also compared to see whether some pipeline systems are more problematic for leak detection than the others.

1.5 Thesis Structure

This thesis is organized in four chapters. Chapter 1 presents the background on pipeline leak detection, challenges faced by computer model based leak detection systems, and previous research about the analysis of uncertainty in water supply networks and energy pipeline systems. In Chapter 2, the methodology used in this project is explained. Chapter 3 presents the results and discussion of the uncertainty study. Conclusions and recommendations are highlighted in Chapter 4.

Chapter 2: Methodology

2.1 Study Pipeline

API 1149 (1993) demonstrated that pipeline systems with the same *R* factor have the same hydraulic response. This allowed the use of one pipeline to conduct tests that were representative of a wide range of pipeline configurations under various operating conditions. A simple study pipeline with one injection and one delivery and no intermediate pump station was designed (Figure 2-1). It is also representative of a pipe segment between two stations for more complicated pipelines with multiple pump stations. The characteristics of the study pipeline were selected based on the pipeline catalogue of 30 plus pipelines provided by the industry partner. The outside diameter of the study pipeline was selected to be 30 inches because it was the pipe diameter that occurred most often (in terms of pipe length). The length was set to 150 km, and the pipe roughness was set to 0.0001. The study pipeline carried a single fluid of crude oil with a density of 858.6 kg/m^3, a viscosity of 4.57 centipoise (cP), and a bulk modulus of 209,800 psi. Temperature effect was excluded from this study by setting a constant temperature of 15 ℃. The effect of gravitational alignment was also eliminated by assuming the pipeline was horizontal with no elevation changes. Flow rate and pressure measurements were available at both upstream and downstream ends.

Systems with different *R* values were shown to have distinctly different hydraulic responses (API 1149, 1993; Pabon, 2015). Systems with high *R* values are friction-dominated thus the transient signal caused by operation or leak attenuates quicker compared to the systems with low *R* values, which are inertia-dominated. To study how different types of hydraulic response affect leak detectability, the initial flow rate in the

study pipeline was adjusted to obtain two systems with different *R* values, a low value of 0.49 (corresponding to a flow rate of 468.2 m^3/hr) and a high value of 2.20 (corresponding to a flow rate of 3121.5 m^3/hr).

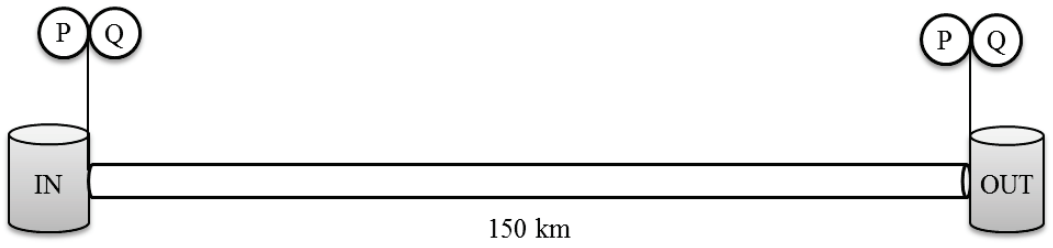

Figure 2-1. Schematic of the study pipeline.

2.2 Simulated Leak Test

Leak detectability can be best evaluated with a fluid withdrawal test, which is the closest representation of leak in a real pipeline system. However, fluid withdrawal tests are not frequently conducted due to high cost and complexity, especially for pipelines with large diameter and high flow rate where the removed fluid is of large quantity and difficult to store (Vinh, 2012). By contrast, a simulated leak test utilizes a computer model to mimic a leak thus is less expensive, easier to conduct, and more flexible for testing various normal or abnormal operating conditions. Figure 2-2 shows the procedure of a real leak detection system versus the simulated leak test system. In the real leak detection system, data are collected from field sensors (e.g. flow meters and pressure transmitters) along the pipeline by the SCADA system and written into an RTU data file. This RTU data file is then used to drive the *real-time transient model* based leak detection system (i.e. *SPS Statefinder* in this study). It can be seen that in the simulated leak test system the computer model is acting the role of the actual pipeline, the field

sensors, and the SCADA system. It produces a simulated RTU data that is in the exact same format as a real RTU data file and is then used to test the response of the same leak detection system.

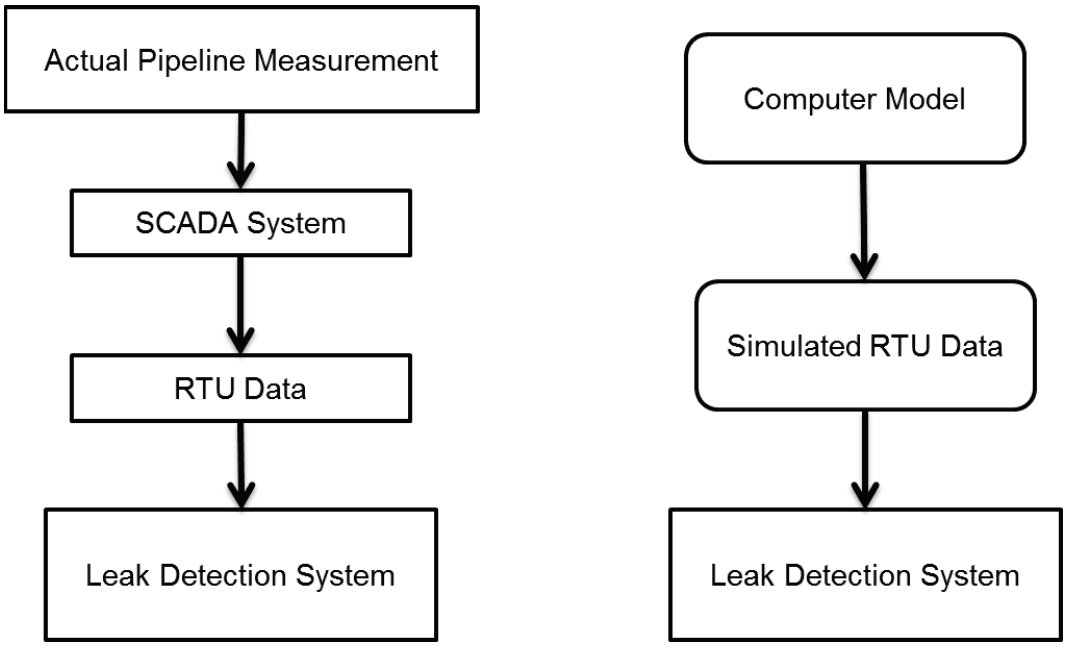

Figure 2-2. Real leak detection system (left) versus the simulated leak test system (right).

A simulated leak test was used in this study to quantify the performance of the leak detection system. The *Simulator* module of the *SPS* software was used to generate the simulated RTU data. The study pipeline was set up in the *Simulator*. Leak was created by opening an imaginary "valve" at the midpoint and letting fluid out of the virtual pipeline into an imaginary tank (Figure 2-3). Leak was set to occur at the midpoint of the study pipeline because it was shown that leak detectability was not very sensitive to leak locations (leak located at 1/4, 1/2, and 3/4 pipe length were compared), according to Pabon (2015), which studied the sensitivity of the leak detection system to selected key

variables. Leak rate was set to a constant value and reached within 2 seconds. Leak sizes tested were 2%, 5%, and 30% of the pipeline flow rate. It was shown that the small leak (i.e. 2%) was often completely masked by uncertainties (results are shown in Appendix B), while large leak (i.e. 30%) was minimally affected (results can be found in Appendix C). Therefore, 5% leak was used to quantify the performance of the leak detection system in this study. For each simulated leak test, an RTU data file was generated by running the *Simulator* model for 8 hours. Leaks were introduced at 4-hour simulation time.

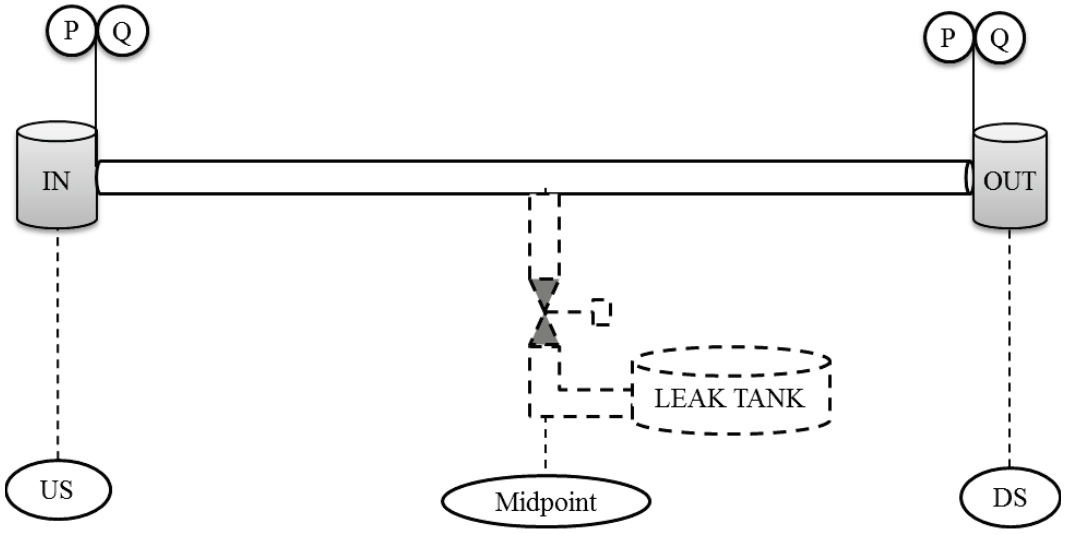

Figure 2-3. Schematic of the virtual pipeline for a simulated leak test.

The injection location of a pipeline is typically equipped with pumps to supply enough pressure head to move the oil; and the delivery location is often equipped a pressure control valve to control the delivery pressure. The pumps and valve were simulated indirectly by controlling pressure or flow rate at the equipment locations instead of directly modelling the pump and valve curves. This method was shown to produce more accurate model results compared to direct modelling of the equipment (API

1149, 1993). Both steady and transient operating conditions were conducted. For steady state, a constant flow rate was specified at the upstream (US) injection location and a constant delivery pressure was controlled at downstream (DS) end. A flow increase transient was created to mimic a pump start at the injection location. The flow rate at US was increased by 50% during 5 seconds while the pressure at DS was held constant. A flow decrease transient was also designed to mimic a valve closure at the delivery location. The pressure at upstream was held constant while the flow rate at DS was decreased by 50% during 5 seconds. Severe transient events in real pipeline systems are often associated with the closure of fast response pressure control valves which can close by 95% within 3-5 seconds (personal communication Enbridge Pipelines, 2013). However, a flow decrease of more than 50% led to column separation in the study pipeline, i.e. pressure drops below vapor pressure and gas vapor bubbles form in the oil. To eliminate this complexity introduced by two-phase flow, flow changes were limited to ±50%. The transient events tested in this study were considered relatively severe compared to what may occur in real pipeline systems. Transient event was introduced into the *Simulator* model at the same time as the leak (4-hour simulation time), as this was shown to be the worst-case scenario for leak detection during transient operations (Pabon, 2015).

RTU data generated by *Simulator* were free of sensor noise, which was referred to as “perfect data” in this study. To better mimic the real-world RTU data, Gaussian distributed noise was generated and added to the simulated leak data using a noise generation tool developed in MATLAB. Noise levels tested were 1% and 2% of the pressure and flow rate values. The modified RTU data containing Gaussian noise were

referred to as “noisy data” in this study. Figure 2-4 shows an example of perfect data and noisy data mimicking a flow meter measurement. Both perfect data and noisy data were used to drive *SPS Statefinder* when evaluating the performance of the leak detection system.

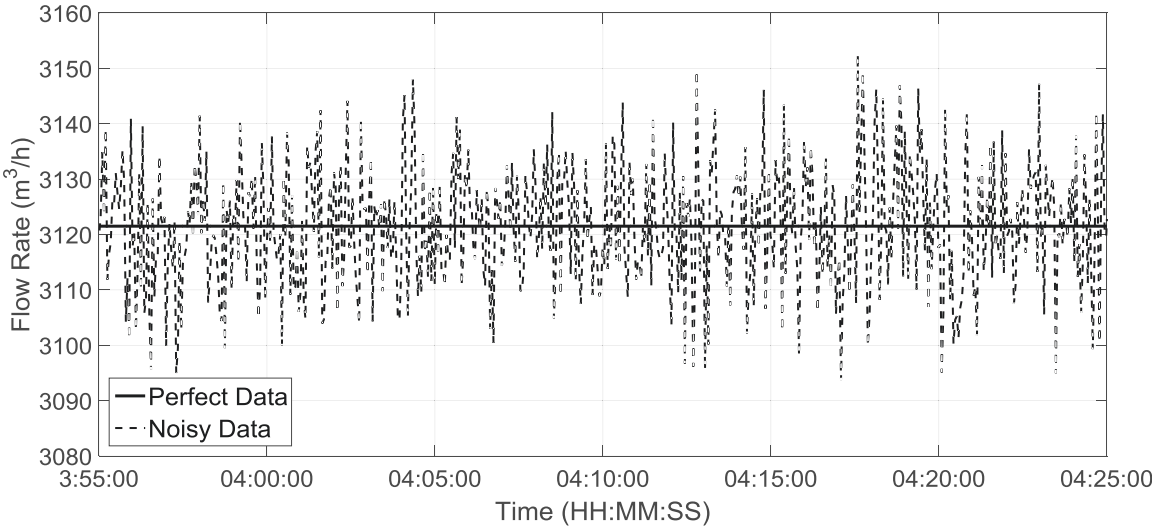

Figure 2-4. A comparison between perfect data and noisy data.

2.3 Leak Detection System

The leak detection system *SPS Statefinder* consists of two main parts, a real-time transient hydraulic model and a leak detection algorithm named state estimation (DNV-GL SPS Help and Reference Manual, 2012). The hydraulic model estimates the pipeline state by solving the conservation equations of the pipe flow, assuming the pipeline system is free of leak. The equations of mass and momentum conservation can be expressed as,

$$\frac{1}{\rho a^2}\left(\frac{\partial P}{\partial t}+V\frac{\partial P}{\partial x}\right)+\frac{\partial V}{\partial x}=0 \tag{2-1}$$

$$\frac{1}{\rho}\frac{\partial P}{\partial x}+V\frac{\partial V}{\partial x}+\frac{\partial V}{\partial t}+\frac{fV|V|}{2D}+g\sin\alpha=0 \tag{2-2}$$

where P is the pressure (Pa); V is the flow velocity (m/s); ρ is the density of the fluid (kg/m^3); f is the Darcy-Weisbach friction factor (dimensionless); g is the gravitational acceleration (m/s^2); α is the upward angle between the pipe and the horizontal (degree); x is distance (km); t is time (s); D is the pipe diameter (m); and a is the wave speed of the pipeline system (m/s) given by

$$a = \frac{\sqrt{K/\rho}}{\sqrt{1+\frac{KD}{Ee}}} \tag{2-3}$$

where e is the pipe thickness (m), E is Young's modulus, and K is bulk modulus. Both have the unit of pressure, which is Pa in SI unit and psi in IM unit. Bulk modulus is defined as

$$K = -\tilde{V}\frac{dP}{d\tilde{V}}$$

where $\tilde{V}$ is the volume of the fluid (m^3) (Wylie and Streeter, 1993).

For a simple pipeline with one injection and one delivery point, it is sufficient to determine the hydraulic state if one boundary condition is provided at each pipe end, as long as all the input parameters to the model precisely describe the actual pipeline system. Any other measured data would be redundant for estimating the hydraulic state. However, real-world uncertainties can never be avoided. Uncertainties in fluid properties, pipe configuration, and data can all contribute to discrepancies between modelled and measured hydraulic state. The state estimation algorithm optimizes the pipeline state (e.g. pressure, flow rate, and friction factor) to reasonably ascribe the discrepancies to real-world errors and/or leaks by making best use of all available measurements.

State estimation adjusts measured pressures and flow rates, pressure drops, and wave speed, as well as removing or adding fluid from the pipeline. A penalty (E) is

assigned for each adjustment being made as seen in the following equations (only showing terms relevant to this study) and the solution that minimizes the sum of all the penalties is sought (DNV-GL SPS User Manual, 2012).

$$E_1 = \sum_i \left(\frac{W_1}{REP_i^P} \times \left(P_i^M - P_i^A \right) \right)^2 + \sum_i \left(\frac{W_2}{REP_i^Q} \times \left(Q_i^M - Q_i^A \right) \right)^2 \quad (2\text{-}4)$$

E_1 is the penalty associated with the errors in measured pressure and flow rate, where P_i^M and Q_i^M are measured pressure and flow rate at sensor location *i,* P_i^A and Q_i^A are the adjusted pressure and flow rate used in the model, (P_i^M - P_i^A) and (Q_i^M - Q_i^A) are the amount of adjustments state estimation made to the measured pressure and flow rate, REP_i^P and REP_i^Q are the repeatability of the pressure transmitters and flow meters, i.e. the estimated errors in the measured pressure and flow rate, W_1 and W_2 are the tuning weights assigned to pressure measurements and flow rate measurements respectively. A smaller weight indicates a higher level of uncertainty and *Statefinder* is less penalized for making adjustments to the relevant variables (DNV-GL SPS User Manual, 2012).

$$E_2 = \sum_i (W_3 \times FPDC_i)^2 \quad (2\text{-}5)$$

E_2 is the penalty associated with the errors in modelled pressure drop caused by friction, W_3 is the tuning weight assigned to friction, $FPDC_i$ is a correction coefficient applied to the friction factor *f* of pipe segment *i*. It is applied to the friction factor *f* of a pipe segment,

$$f_c = (1 - FPDC) \times f \quad (2\text{-}6)$$

where *f* is the friction factor in the model calculated by Colebrook method with the input viscosity, and f_c is the friction factor after state estimation adjusts it. The bound of *FPDC* is ±15%, augmented by a user-defined parameter, *Viscosity·Error (VER)* (DNV-GL SPS

User Manual, 2012). *VER* can be increased so that full correction can be made to friction factor.

$$E_3 = \sum_i \left(\frac{W_4}{1000 \times \Delta t} \times \left(P_i^A - P_{i,prev}^A \right) \right)^2 + \sum_i \left(W_5 \times \left(FPDC_i - FPDC_{i,prev} \right) \right)^2 + \sum_i \left(\frac{W_6}{BMC_{a,i}} \times \left(BMC_i - BMC_{i,prev} \right) \right)^2 \quad (2\text{-}7)$$

E_3 is the penalty associated with the errors in the rate of change of the modelled pressure, the friction correction coefficient, and the bulk modulus correction coefficient *BMC*. Δt is the time step and the subscript *prev* represents values used at the previous time step; W_4, W_5, and W_6 are the tuning weights assigned to the rate of change of pressure, friction, and bulk modulus respectively; $BMC_{a,i}$ is the maximum allowed bulk modulus correction coefficient in the simulation; *BMC* is applied to the wave speed:

$$a_c^2 = a^2 \times (1 - BMC) \quad (2\text{-}8)$$

where a is the calculated wave speed with the input bulk modulus and a_c is the wave speed after correction. The bound for *BMC* is set by a user-defined parameter *BMER* and cannot exceed 0.5 (DNV-GL SPS User Manual, 2012).

$$E_4 = \sum_i (W_7 \times DF_i)^2 \quad (2\text{-}9)$$

E_4 is the penalty associated with the error that cannot be attributed to the real world uncertainties thus may be induced by a leak and W_7 is the corresponding tuning weight. DF_i is defined as "diagnostic flow" in pipeline segment i in *Statefinder*. If negative, it indicates removal of fluid from the modelled pipeline (DNV-GL SPS Help and Reference Manual, 2012). Leak detection is often based on volume imbalance, which is calculated by integrating the diagnostic flow *(DF)* over a period of time, or time window. Volume imbalance is typically monitored by integrating over different time intervals referred to as

time windows (e.g. 5 minutes, 1 hour, and 24 hours), with smaller windows targeted to detect large leaks quicker and larger windows targeted to detect smaller leaks (Canadian Standard Association Z662 Annex E). This is because over a short period of time, it is very difficult to distinguish a leak from the volume imbalance caused by uncertainties; whereas in a longer time window, the volume imbalance caused by the leak steadily increases and becomes distinguishable. In this study, volume imbalance in a one-hour time window was used to quantify leak detectability according to the 5% leak size. A dimensionless volume imbalance (*DVB*) was defined as volume imbalance divided by the leak volume (the volume of fluid leaked out over an hour). This allowed different testing scenarios with different sizes of leaks to be compared.

The objective function to be minimized is the summation of all the penalties listed above. The decision variables are the pressure measurement, flow rate measurement, *FPDC*, and *BMC*. The constraints for the pressure and flow rate measurements are the repeatability of the field sensors. *FPDC* bound and *BMC* bound exert constraints to *FPDC* and *BMC* respectively. At each time step, state estimation seeks the values of the decision variables to obtain the minimal objective function, which indicates a best fit between the modelled and actual pipeline state.

2.4 Sources of Uncertainty

Uncertainties are often present in fluid properties, field sensors, and SCADA systems, thus they were evaluated in this study. Properties of a fluid are often not known accurately since fluids with different properties may be mixed in tanks before injection into the pipeline. As a result, density, viscosity, and bulk modulus can differ greatly from

the nominal value measured in the laboratory. In the actual pipeline systems, the density of a fluid is often measured by a densitometer before injection. However, viscosity and bulk modulus are typically not measured on the pipeline and the values measured periodically in the laboratory are used in the leak detection system. The impact of inaccurate viscosity and bulk modulus were assessed by purposely setting wrong values for these two variables in the hydraulic model of the leak detection system. Viscosity was varied to introduce a ±20% in the *R* factor through the friction factor (*f*). Initially bulk modulus was also varied to introduce a ±20% error to the *R* factor through the wave speed (*a*). This was conducted to see whether viscosity error and bulk modulus error would have the same impact on leak detection if they both cause exactly the same level of uncertainty in the *R* factor. However, ±20% error in the *R* factor resulted in unrealistically large error in the bulk modulus. Therefore, the realistic level of uncertainty (±10%) in bulk modulus was also tested (personal communication Enbridge Pipelines, 2016). The values of viscosity and bulk modulus tested are shown in Table 2-1.

Table 2-1. Level of uncertainties in fluid properties.

	Variable Value			Equivalent Error in *R*		
	Lower	Base	Upper	Lower	Base	Upper
Viscosity *R* = 2.20 (cP)	1.31	4.57	11.53	-20%	0	+20%
Viscosity *R* = 0.49 (cP)	1.69	4.57	9.85	-20%	0	+20%
Bulk modulus realistic (psi)	188,820	209,800	230,780	+3.5%	0	-3.0%
Bulk modulus large (psi)	124,268	209,800	480,250	+20%	0	-20%

The SCADA system can also contribute to uncertainties. Errors may be introduced because the SCADA system polls data from field sensors at discrete time and

therefore there is uncertainty between the polling intervals. Polling time of 1 second, 5 seconds, and 10 seconds were tested to see whether the loss of important information during transient period could degrade leak detectability. In addition, the SCADA system polls data from each sensor consecutively rather than from all field sensors simultaneously. Field sensors at different locations are polled at different times but stamped at the same time, causing a "time skew". The maximum time skew in real pipeline systems could reach 10 seconds (personal communication Enbridge Pipelines, 2016). For field sensor where the pressure or flow rate was controlled at constant, variation in reporting time does not affect the reported value. For example, the flow rate at upstream end and pressure at downstream end were both held constant for steady state scenarios in this study. Therefore, time skew was introduced to upstream pressure and downstream flow rate as their "measured" data change with time. The scenarios tested are shown in Table 2-2.

Table 2-2. Tested scenarios of time skew.

Flow Condition	Sensors with Time Skew
Steady State (with leak)	Pressure at US point
	Flow rate at DS point
	Pressure at US point & Flow rate at DS point
Flow Decrease	Flow rate at US point
	Flow rate at DS point
	Pressure at DS point
	Flow rate at US point & Pressure at DS point
	Flow rate & Pressure at DS point
Flow Increase	Pressure at US point
	Flow rate at US point
	Flow rate at DS point
	Pressure at US point & Flow rate at DS point
	Flow rate & Pressure at US point

When time skew is present in field sensor(s), additional model parameters are needed,

$$EREP = REP + TEB \times FILP \tag{2-10}$$

where *EREP* is the effective repeatability, which defines the bound within which the measured flow rate or pressure data can be adjusted; *REP* is the sensor repeatability as previously defined; *TEB* is a time tag error bound which is a user-defined parameter associated with time skew. *TEB* was set to zero when there was no time skew in the simulated leak data; and it was set to 10 seconds for the tests with 10-second time skew; *FILP* is the absolute value of the slope between two measured points. It can be seen that

larger time skew causes the increase of *EREP*, and the bound for adjusting the measured flow rate or pressure is larger (DNV-GL SPS User Manual, 2012).

Error was first introduced into each possible source of uncertainty separately including viscosity, bulk modulus, polling time, and time skew. Tests were conducted using both perfect data and noisy data to study the effect of data noise. Errors were then introduced into all sources randomly and the range of uncertainty for each variable is shown in Table 2-4. The tuning weights in equations (2-4), (2-5), (2-7), and (2-9) needed to be set differently for the single error case and the random error case (Table 2-3). When only a single variable contains uncertainty, its corresponding weight was set to a relatively small value compared to the weights for the other terms that contained no error. For example, for tests with viscosity error alone, the tuning weight for *FPDC* (W_3) was set to 1, which was the smallest value among all the tuning weights. W_1 and W_2 were set to 1 in all cases. This is because when "measured" data contains data noise, adjustment to the "measured" data is desirable and *Statefinder* was less penalized for making such adjustment. The bound for the adjustment was determined by the sensor repeatability. For perfect data cases, repeatability of all sensors was set to be zero thus no adjustments to the measured pressures or flow rates would be made regardless the values of W_1 and W_2.

In the cases where error was introduced randomly in any uncertainty sources, the tuning weights were set similar to what are used for real-life pipelines (Table 2-3). Measurements (pressure and flow rate), friction, and bulk modulus were considered the most likely uncertainty sources thus W_1, W_2, W_3, and W_6 were all set to 1. W_7 was set to the second smallest value (5) so that *Statefinder* was less penalized for generating diagnostic flow to account for leak. More penalty was given to the change rate of

pressure and friction by setting W_4 to 10 and W_5 to 500. The purpose of the random uncertainty tests was to statistically analyze the effect of uncertainties on leak detectability. The *MCS* method was used to generate all uncertainty variables, including viscosity, bulk modulus, polling time, time skew (magnitude and location), and data noise level. The range of uncertainty for each variable is listed in Table 2-4. A total of 500 combinations were tested for each flow condition, steady state, flow decrease, and flow increase transient.

Errors were introduced in the various uncertainty sources and the response of the leak detection system as indicated by the one-hour window *DVB* was compared to the baseline case which was error free. A leak alarm threshold was needed to quantify leak detectability. A threshold too large would result in delayed or missed detection of a leak; while a threshold too small would lead to too many false alarms. Therefore, a leak threshold corresponding to a 2% leak was used in this study. When superimposed onto the *DVB* figure (e.g. Figure 3-1a), the 2% threshold appears to be a horizontal line at *DVB* = -0.4 because it was scaled by the volume of fluid leaked out of the pipeline over one hour for a 5% leak. The interception of the threshold line and the *DVB* curve indicates the time when a leak was detected, which are marked out with arrows in the figure.

Table 2-3. Tuning weights in *Statefinder* for single error and random error scenarios: W_j (j = 1-7) are weights assigned to measured pressure and flow rate, friction, rate of change of pressure, friction, and bulk modulus, and diagnostic flow, respectively.

Tuning Weights	Viscosity	Bulk Modulus	SCADA	Random Error
W_1	1	1	1	1
W_2	1	1	1	1
W_3	1	10^7	10^7	1
W_4	10	10	10	10
W_5	500	10^7	10^7	500
W_6	10^7	1	10^7	1
W_7	5	5	5	5

Table 2-4. The range of uncertainty for each variable in random error tests.

Variables	Range of Uncertainty
Viscosity	1.31cP - 11.53cP
Bulk Modulus	188,820 psi - 230,780 psi
Data Noise	1%, 2%
Time Skew	5s, 10s
Polling Time	5s, 10s

Chapter 3: Results and Discussion

3.1 Single Error Source

3.1.1 Uncertainty in *R* Factor

The effect of uncertainty in the *R* factor, caused by errors in the different variables it comprises, was first evaluated. A ±20% error was introduced in the *R* factor by varying the viscosity or bulk modulus as listed in Table 2-1. For all cases, *Statefinder* was configured to allow for adjustment of the viscosity or bulk modulus to their correct values. This was achieved by adjusting the bounds of *FPDC* and *BMC*.

Figure 3-1 shows the results with perfect data. It can be seen that leak detectability was not affected by the viscosity error as the *DVB* baseline and the positive and negative viscosity error curves overlap precisely onto each other. However, this was not the case when the uncertainty in the *R* factor was introduced by an incorrect bulk modulus. For flow decrease (Figure 3-1a), the detection time for the baseline case was 24.9 minutes after the leak started at 4:00:00. The curve of the 120% *R* case deviated from the baseline and detection of the leak was delayed by 11.5 minutes, a 46% increase in detection time; whereas, the -20% error in *R* caused by bulk modulus (80% *R* case) did not affect leak detectability, i.e. its *DVB* curve collapsed onto the baseline. During flow increase (Figure 3-1b), the detection time was also delayed for the 120% *R* case, but for the 80% *R* case, the *DVB* curve did not collapse exactly with baseline as under flow decrease condition. The detection time was slightly earlier by 1.7 minutes. Steady state (Figure 3-1c) was much less affected by bulk modulus error than during transient operating conditions. Similar trend was observed with noisy data (Figure 3-2). Leak detectability was not affected by the viscosity error, but was affected by bulk modulus

error, particularly during transient operating conditions. The changes in detection time due to bulk modulus error as well as the corresponding baseline detection time are summarized in Table 3-1. Only results for system with $R = 2.20$ are shown because the findings are similar for the system with $R = 0.49$ (results can be found in Appendix A).

These results evidently show that the viscosity error and bulk modulus error have different effects on leak detectability, even though they both introduced exactly the same amount of error in the R factor. Viscosity error did not affect leak detectability while the impact of bulk modulus error could be significant. Therefore, the effect of the uncertainties in individual variables comprising the R factor must be evaluated individually. This is a different finding from API 1149 (1993), which concluded that uncertainty in different variables comprising the R factor has equal impact on leak detectability. This is likely due to the different leak detection methods employed in API 1149 and this study.

Table 3-1. Changes in detection time for ±20% uncertainty in the R factor caused by bulk modulus error ($R = 2.20$)

Data Type	Flow Condition	Baseline Detection Time (minutes after leak start)	Change in Detection (min)	
			120% R	80% R
Perfect Data	Flow Decrease	24.9	11.5	0
	Flow Increase	26.1	14.3	-1.7
	Steady State	25.5	-1.2	1
Noisy Data	Flow Decrease	33.1	17.6	-5.9
	Flow Increase	61.7	17.8	-26.7
	Steady State	41.7	-1.5	1.4

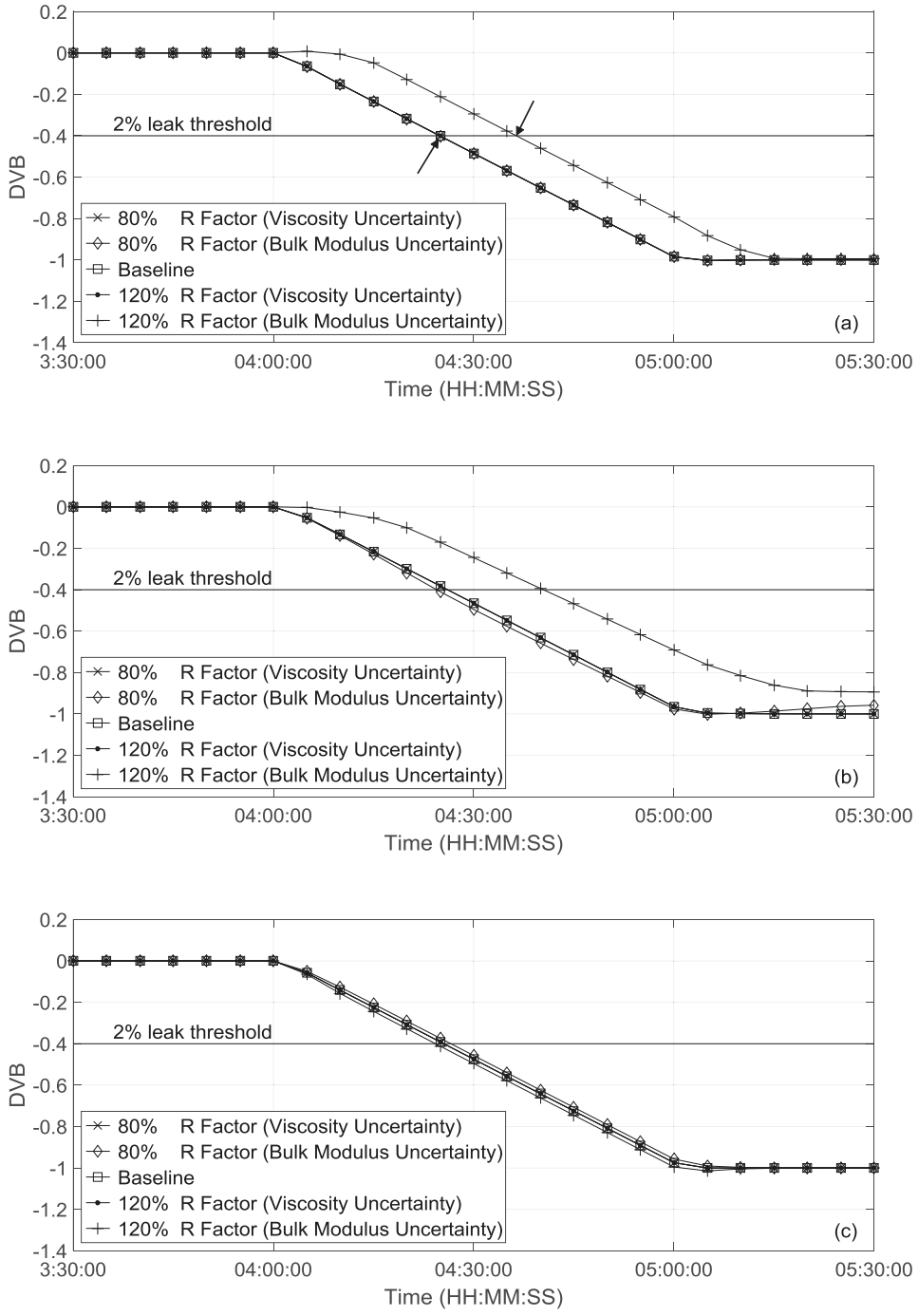

Figure 3-1. Effect of uncertainty in the *R* factor on leak detectability in system of *R* = 2.20 with perfect data: a) flow decrease; b) flow increase; c) steady state. Arrows in a) indicate the interception points between the threshold line and the *DVB* curves.

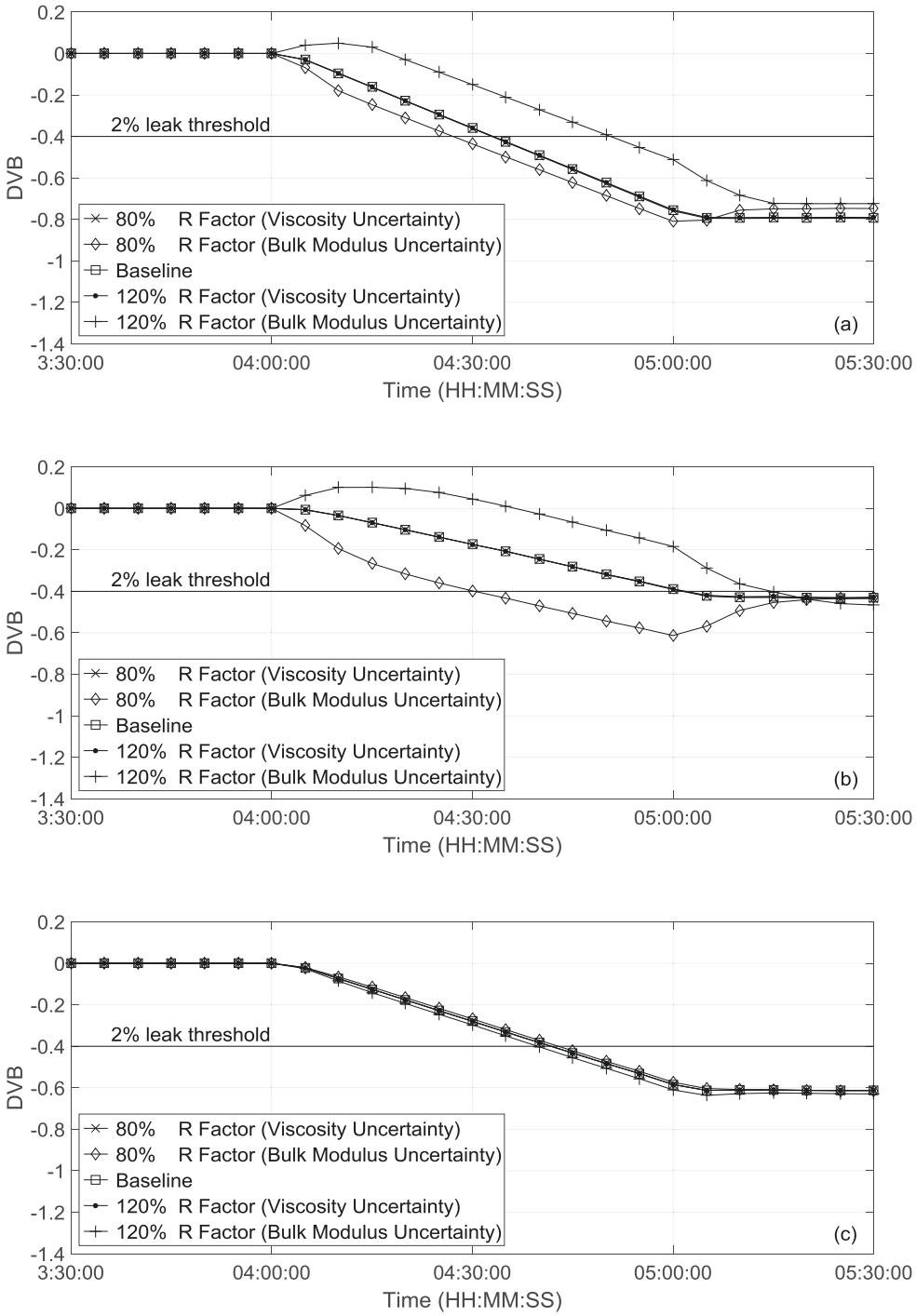

Figure 3-2. Effect of uncertainty in the *R* factor on leak detectability in system of *R* = 2.20 with 1% random noise: a) flow decrease; b) flow increase; c) steady state.

3.1.1.1 Viscosity Uncertainty

In *Statefinder*, the friction correction coefficient *FPDC* is applied to the friction factor *f* of a pipe segment as shown in Equation (2-6). As a result, the 120% *R* (i.e. 120% *f*) case required an *FPDC* of 0.1667 while the 80% *R* (i.e. 80% *f*) case required an *FPDC* of -0.25 in order to adjust the friction factor to the correct value. Therefore, the 80% *R* case required more correction than the 120% *R* case in order to make full correction. The bound for *FPDC* is adjusted by changing *VER*.

It was shown in Figure 3-1 and 3-2 that leak detectability was unaffected by viscosity error if *Statefinder* was allowed to adjust the friction factor to the correct value, i.e. the bound for *FPDC* was set bigger than the required *FPDC*. To further investigate how viscosity errors are handled, *VER* was set to 50% which increased the *FPDC* bound from ±0.15 to ±0.23. This allowed full correction for the 120% *R* case but not for the 80% *R* case. It was found that in both cases the error in the viscosity did not impact leak detectability when simulated leak data was perfect. The three *DVB* curves collapsed exactly onto each other thus the figure is not shown here. However, when 1% noise was present in the pressure and flow rate, Figure 3-3 shows that the *DVB* curve for the 120% *R* case collapsed onto the baseline, while the curve for the 80% *R* case deviated from the baseline indicating that leak detectability was affected when the error in viscosity was not fully corrected. In the latter case, the leak was detected 1.1, 8.5, and 1.1 minutes sooner compared to the baseline detection time of 33.1, 61.7, and 41.7 minutes during flow decrease, flow increase, and steady state respectively. This improved leak detectability caused by viscosity error may not be desirable since the resulting larger diagnostic flow (greater absolute magnitude) was not due to the leak, but rather due to the uncorrected

error in viscosity. The change in detection time was minor since the *FPDC* bound (±0.23) was close to the required correction (-0.25). Smaller bound would lead to further change in detection time.

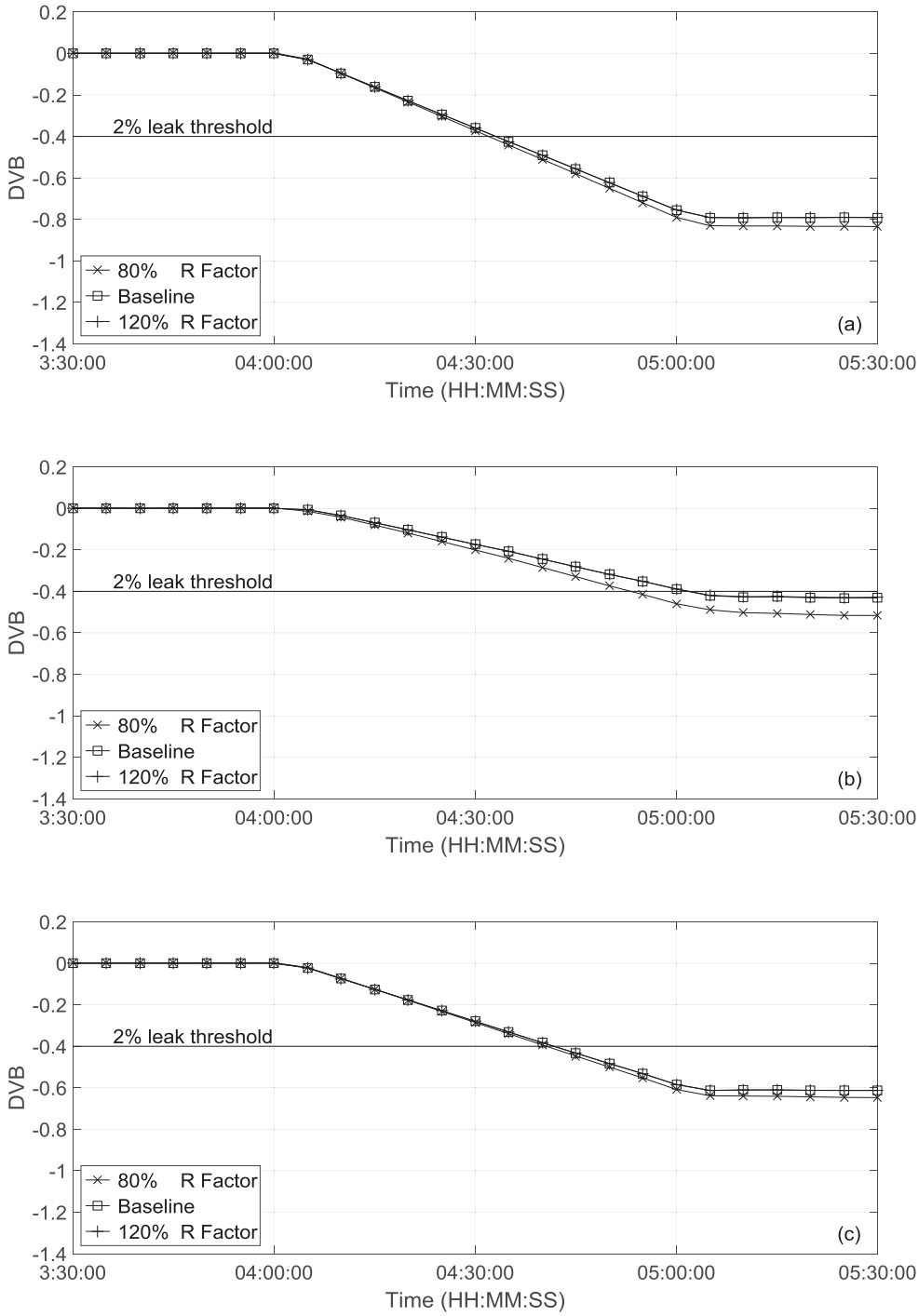

Figure 3-3. Effect of viscosity error on leak detectability in system of R = 2.20 with 1% random noise: a) flow decrease; b) flow increase; c) steady state.

3.1.1.2 Bulk Modulus Uncertainty

As previously shown with the *R* factor test in Figure 3-1 and 3-2, bulk modulus error can have a significant impact on leak detectability. Therefore, the response of the leak detection system to this uncertainty was further investigated with realistic errors of ±10% in bulk modulus. It was found that bulk modulus error only marginally affected leak detectability during steady state operating condition. This is because the error in bulk modulus results in error in wave speed, which only affects transient cases and the transient wave caused by a small leak (e.g. 5% leak) was of small magnitude. Leak detection times changed by less than ±1% compared to the baseline case with either perfect data or noisy data when bulk modulus correction was disabled in *Statefinder* (Figure 3-4). Therefore, only results under transient operating conditions are discussed here.

For all transient cases, *Statefinder* was configured to allow full correction to the bulk modulus error. The correction coefficient *BMC* is applied to the wave speed instead of bulk modulus and is limited by *BMER*. According to equation (2-8) *BMER* needed to be 0.058 for the 110% bulk modulus case and 0.071 for the 90% bulk modulus case to allow full correction. Figure 3-5 shows the effect of bulk modulus errors on leak detectability with perfect data. For the 110% bulk modulus case, the *DVB* curve collapsed onto the baseline curve. However, for the 90% bulk modulus case, the *DVB* curve deviated from the baseline even though full correction was allowed. The leak was detected 4.9 and 7.0 minutes later than the baseline detection time of 24.9 and 26.1 minutes for flow decrease and increase transients, respectively.

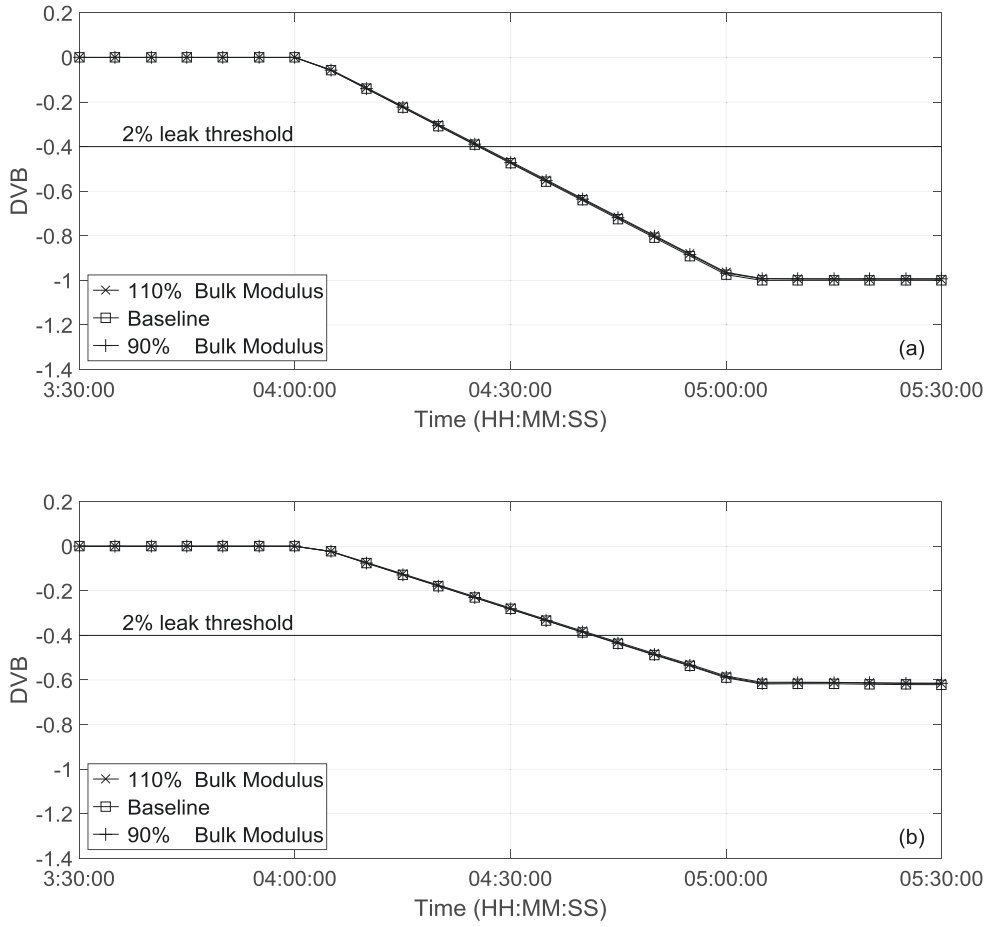

Figure 3-4. Effect of bulk modulus error on leak detectability in system of $R = 2.20$ during steady state (*BMC* disabled): a) perfect data; b) noisy data (1% random noise).

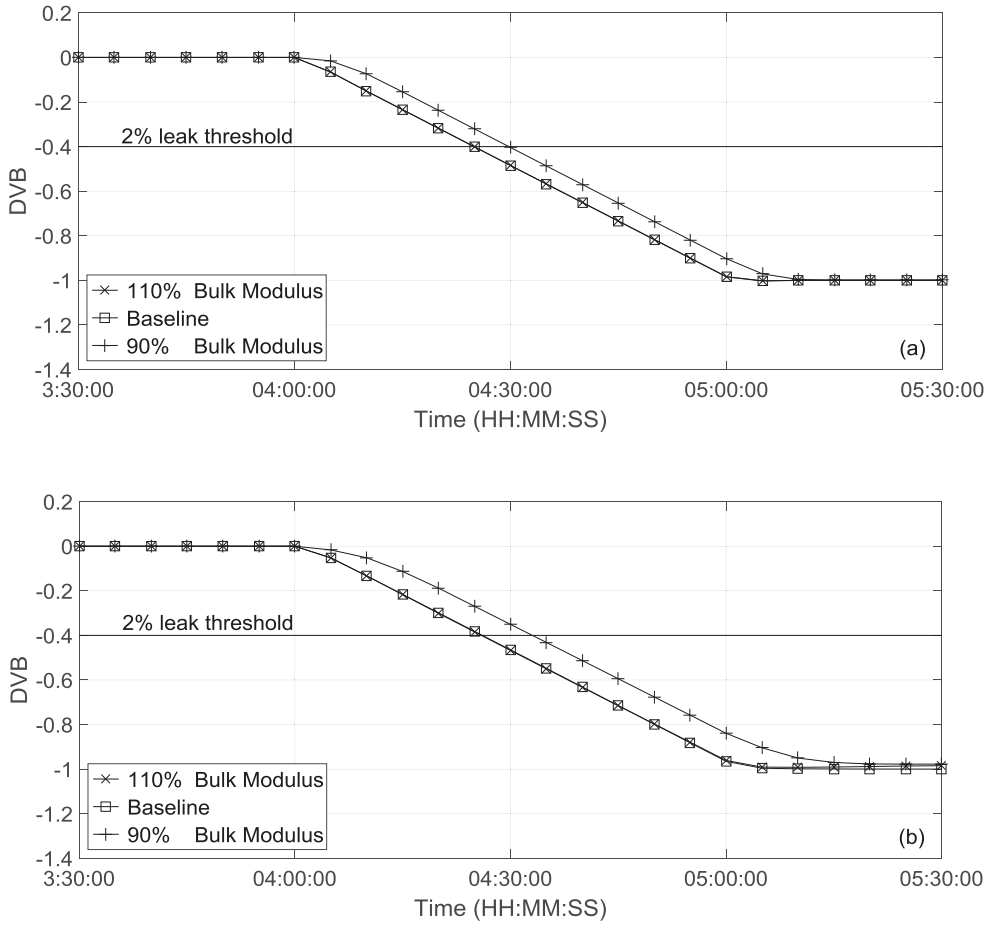

Figure 3-5. Effect of bulk modulus error on leak detectability in system of $R = 2.20$ with perfect data: a) flow decrease; b) flow increase.

To determine the reason why the *DVB* curve for the 90% bulk modulus case deviated from the baseline case even when full correction was allowed, the behavior of the bulk modulus correction coefficient *BMC* was investigated. It was observed that the sign of *BMC* did not always depend on whether the bulk modulus contained positive or negative errors. In Figure 3-6a the *BMC* is plotted for the 90% bulk modulus case for the flow decrease transient in the system of $R = 2.20$. Despite the fact that the bulk modulus required a positive correction, the sign of *BMC* was positive (which would correspond to a negative correction in the bulk modulus) for a significant period of time. Since

Statefinder does not output the computed wave speed, it is difficult to explain the observed *BMC* behavior with certainty. However, a logical explanation is that the sign of *BMC* is dependent upon the nature of wave propagations in the pipeline. The changes in pressure at the downstream end with and without leak are also shown. The flow decrease transient at the downstream end caused the pressure to increase and the two pressures (i.e. 0% and 5% leak) overlapped until the leak caused transient arrived at the downstream end. *BMC* was negative up to this point in time and wave speed was adjusted correctly. After this time the pressure with leak increased slower than if there was no leak. *BMC* was positive all the way until a new steady state was achieved, except for a couple of instances where it spiked to a negative value briefly. The positive *BMC* corresponds to a decrease in bulk modulus and wave speed, which is clearly incorrect. In contrast, Figure 3-6b plots the *BMC* for the 110% bulk modulus case. A flow decrease transient was introduced at the upstream end which caused the pressure to decrease. Despite the fact that the bulk modulus required a negative correction, the negative *BMC* corresponds to an increase in the bulk modulus and wave speed, which is also clearly incorrect.

In the low *R* system, the pressure increased and decreased a few times before reaching a new steady state due to wave reflection at the two pipe ends. The finding was in agreement with those for the high *R* system. In general, the sign of *BMC* was positive when the pressure was decreasing and was negative when the pressure was decreasing. As a result, leak detectability in the system with $R = 0.49$ was worse for the case where the bulk modulus error can be properly corrected in the system with $R = 2.20$, but better for the case where the bulk modulus error was incorrectly adjusted in the system with $R = 2.20$ (Table 3-2). The same relationship between the sign of *BMC* and pressure was

observed for flow increase transient. In conclusion, *Statefinder* determines the sign of *BMC* based on wave propagation, rather than on whether the error in the input bulk modulus is positive or negative.

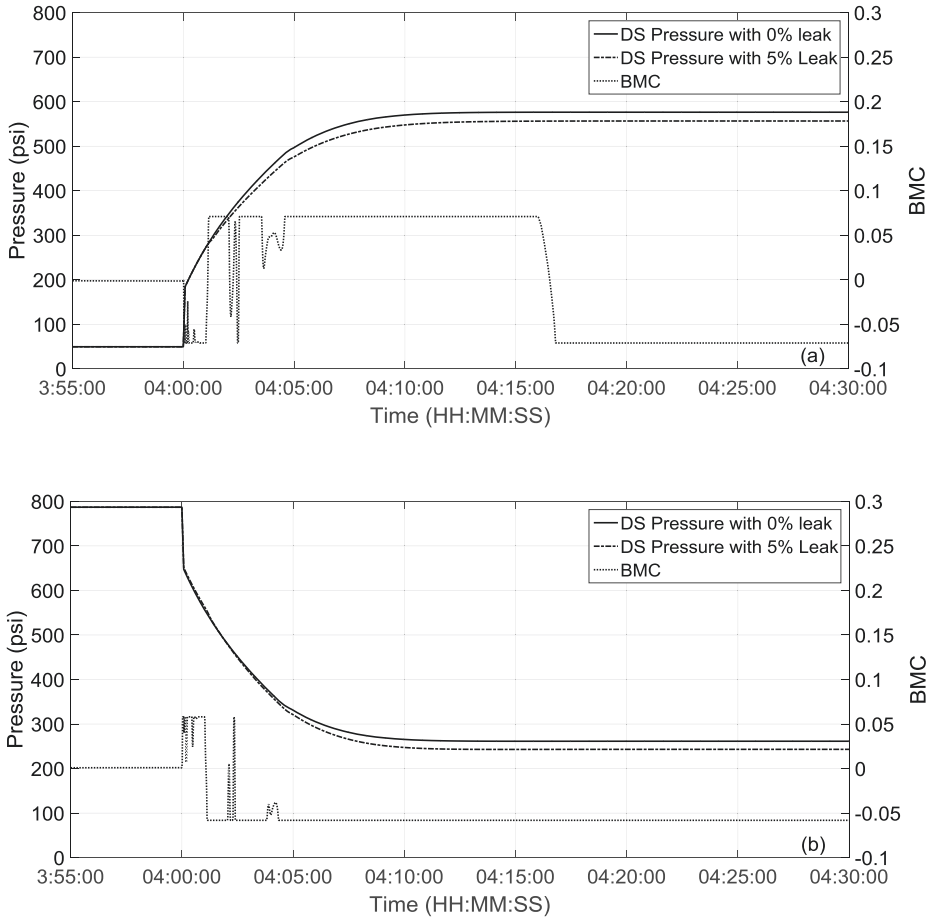

Figure 3-6. *BMC* behavior for flow decrease transient initiated at a) downstream end; b) upstream end in system of *R=2.20* with perfect data.

In addition, it was found that the exact amount of required correction must be specified in order for *Statefinder* to make full correction to bulk modulus. This can be shown with Figure 3-7. Two cases were tested, both with +10% bulk modulus error (110% bulk modulus), but the allowable correction (*BMER*) was set to be exactly the amount needed (0.058) in one case and larger (0.2) in the other case. It can be seen that the *DVB*

curve for the case with the larger *BMER* deviated from the other case and the baseline. The detection time was delayed for 4.8 minutes compared to the detection time of 25.5 minutes for the baseline case. Therefore, if the allowable correction is set too large, *Statefinder* would use it up and make an over-correction to the wave speed, resulting in degraded leak detectability. This is unlike the case with viscosity uncertainty, for which errors can be corrected properly as long as the maximum allowable correction was set greater than the amount of required correction. It is therefore more important to have accurate bulk modulus information than accurate measurement of viscosity.

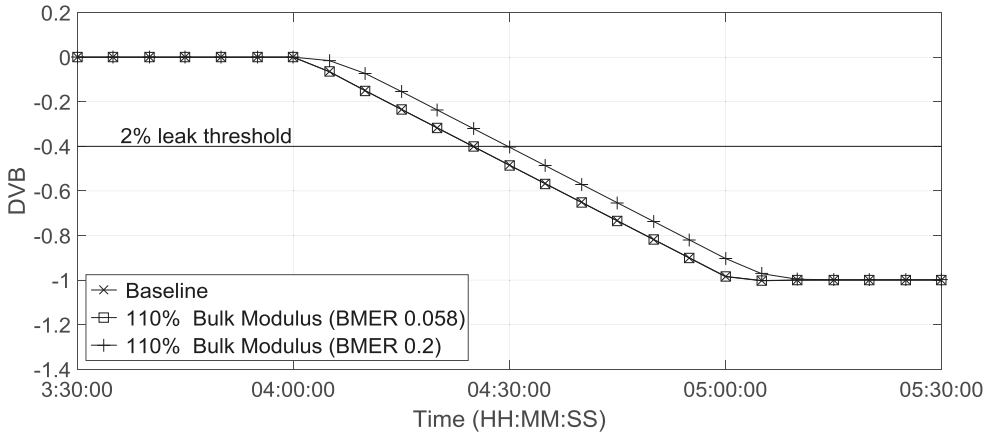

Figure 3-7. Effect of bulk modulus error on leak detectability with exact and excessive *BMER*, in system of $R = 2.20$ with perfect data.

A similar trend was observed with noisy data, as shown in Figure 3-8. The leak detection was delayed for the 90% bulk modulus cases because *Statefinder* made an incorrect adjustment (i.e. incorrect sign) to the bulk modulus. The detection time was delayed 4.9 and 7.1 minutes from the 33.1 and 61.7 minutes for the baseline case for the flow decrease and flow increase transients respectively. The 110% bulk modulus cases were less affected than the 90% bulk modulus cases but did not exactly overlap with the

baseline. The detection time was early by 1.0 and 4.6 minutes for the flow decrease and flow increase transients, respectively. This was because the *BMC* value was oscillating due to the presence of random noise, thus exact correction could not be applied.

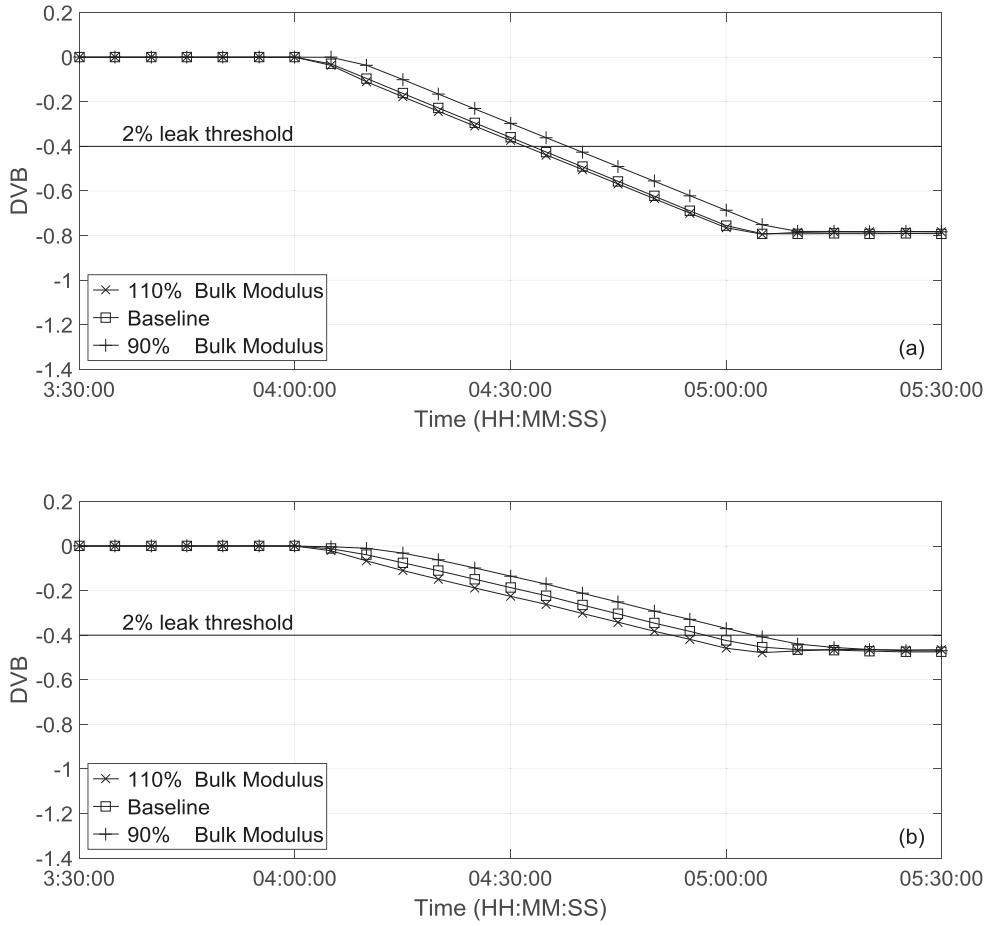

Figure 3-8. Effect of bulk modulus error on leak detectability in system of $R = 2.20$ with 1% random noise: a) flow decrease; b) flow increase.

3.1.2 Uncertainty in Time Skew

When time skew is present in the measured data, false diagnostic flow can be produced even when there is no leak (Figure 3-9). It can be seen that there is a false negative diagnostic flow about 5% of line rate for flow decrease, a false positive diagnostic flow about 50% for flow increase, and no false diagnostic flow for steady state.

Therefore, the leak detection system needs to be configured to increase the *EREP* in order to avoid false leak alarms. *Statefinder* is then allowed to adjust the measured flow rate or pressure by a greater amount. The *EREP* is calculated according to equation (2-10), in which *TEB* was set to 10 seconds corresponding to the 10-second time skew.

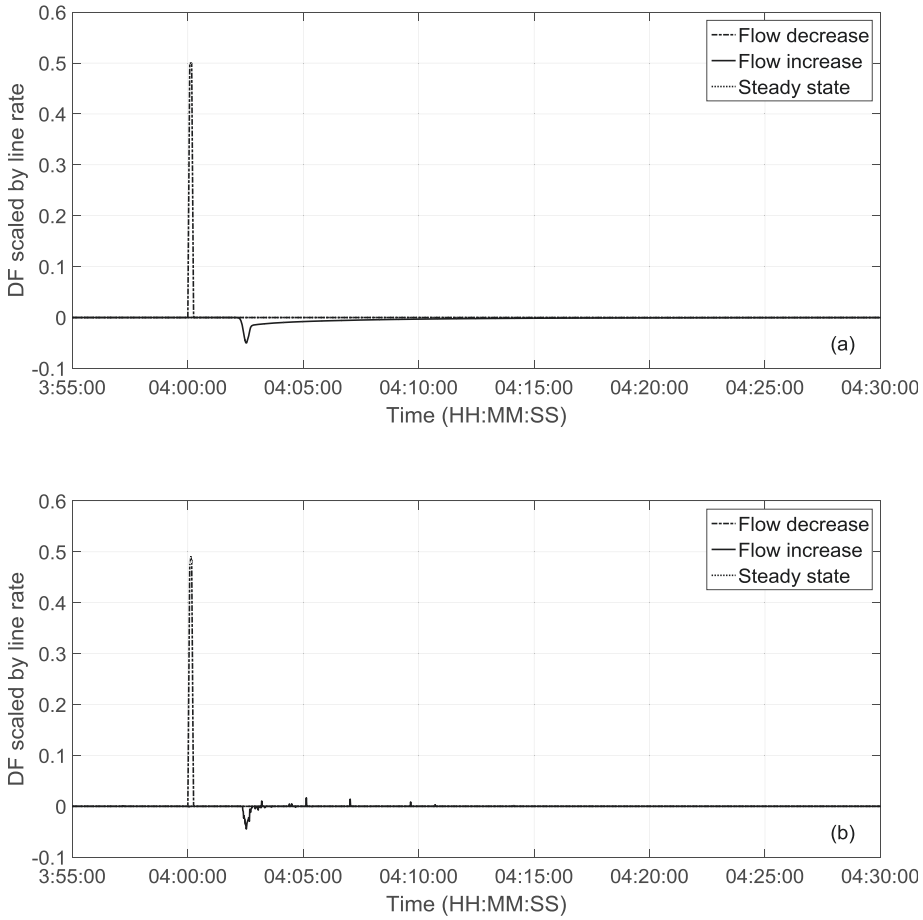

Figure 3-9. False diagnostic flow caused by time skew in system of $R = 2.20$ with no leak: a) perfect data; b) noisy data (downstream flow contained 10 seconds time skew).

In Figure 3-10 *DVB* curves are plotted for cases with 10-second time skew in one or two sensors and no time skew in the remainder during transient and steady state with perfect data. It can be seen that the detection time for transient tests was delayed slightly for all these scenarios, ranging from 0.5 to 3.3 minutes (Figure 3-10a and b) compared to

the baseline case. The detection time for the corresponding baseline case was 24.9 and 26.1 minutes during flow decrease and flow increase transients, respectively. It was also noticed that the delay in detection time was greatest for the cases with time skew in both sensors located at the transient initiation location. When the flow was decreased at the downstream end, the case with time skew in both the downstream pressure and flow rate sensors located at the downstream end experienced the biggest delay of 3.1 minutes; The flow was increased at the upstream end for the flow increase transient and the case with time skew in the upstream pressure and flow rate sensors had the largest delay of 3.3 minutes. Note that leak detection times during steady state operations with perfect data were not affected by time skew (Figure 3-10c). The delay in detection time was more pronounced in the cases with noisy data, as can be seen in Figure 3-11. Time skew had a large impact on leak detectability during both steady state and transient operating conditions. Leak detectability was greatly degraded for noisy data because *FILP* (the slope between two adjacent points in the measured data series) in equation (2-10) was much larger when data noise was present, increasing the *EREP* greatly. Therefore, the bound for adjusting "measured" data is much larger with noisy data cases. Leak detection was delayed by 35 minutes compared to the baseline case detection time 33.1 minutes during flow decrease (Figure 3-11a). For flow increase and steady state cases, leak became undetectable as compared to the detection time of 61.7 and 41.7 minutes for the corresponding baseline cases (Figure 3-11b and c). *DVB* eventually stabilized at -0.08 and -0.22 for the flow increase and steady state cases, both were above the threshold.

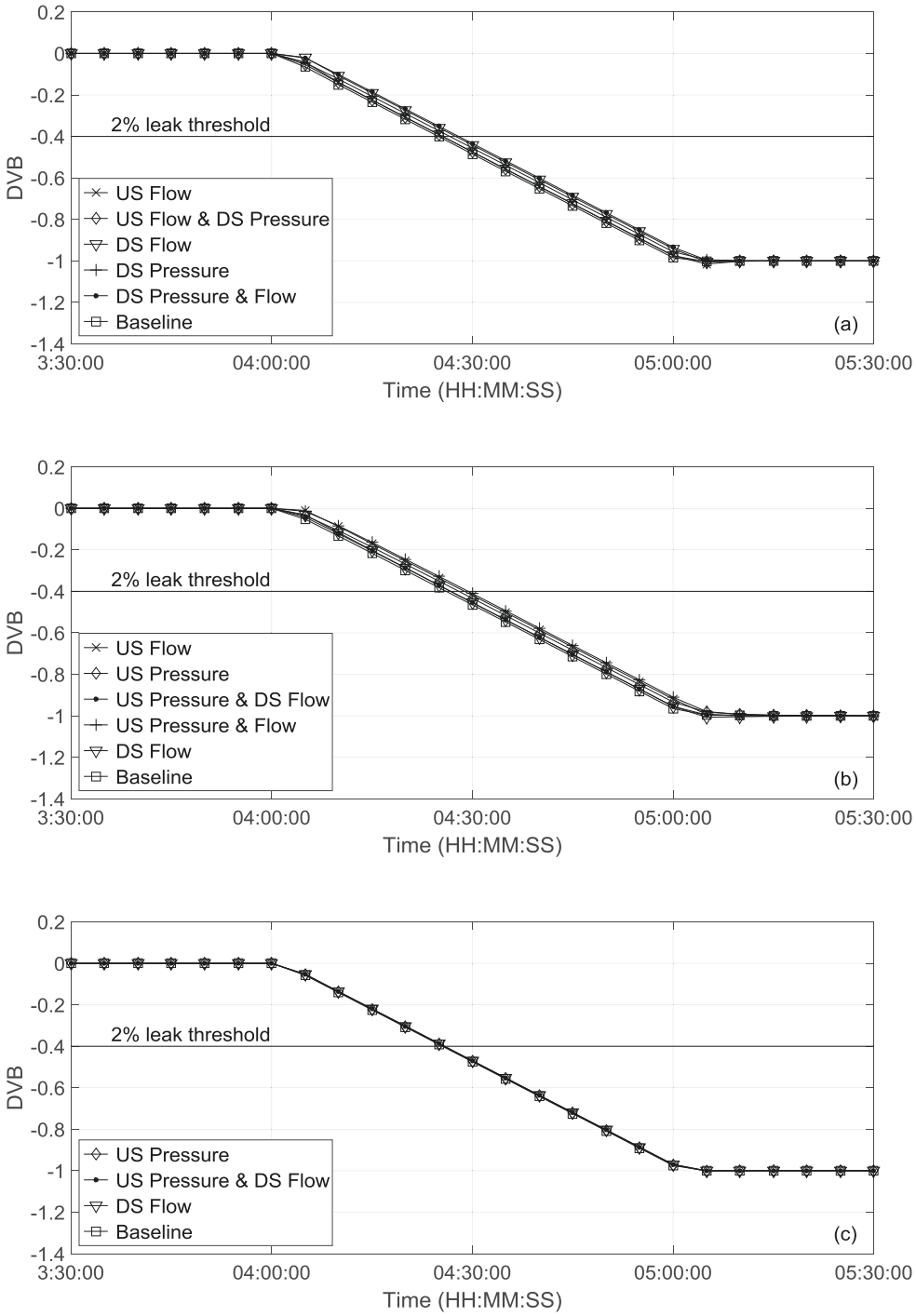

Figure 3-10. Effect of time skew on leak detectability in system of R = 2.20 with perfect data (sensors contain 10 seconds time skew): a) flow decrease; b) flow increase; c) steady state.

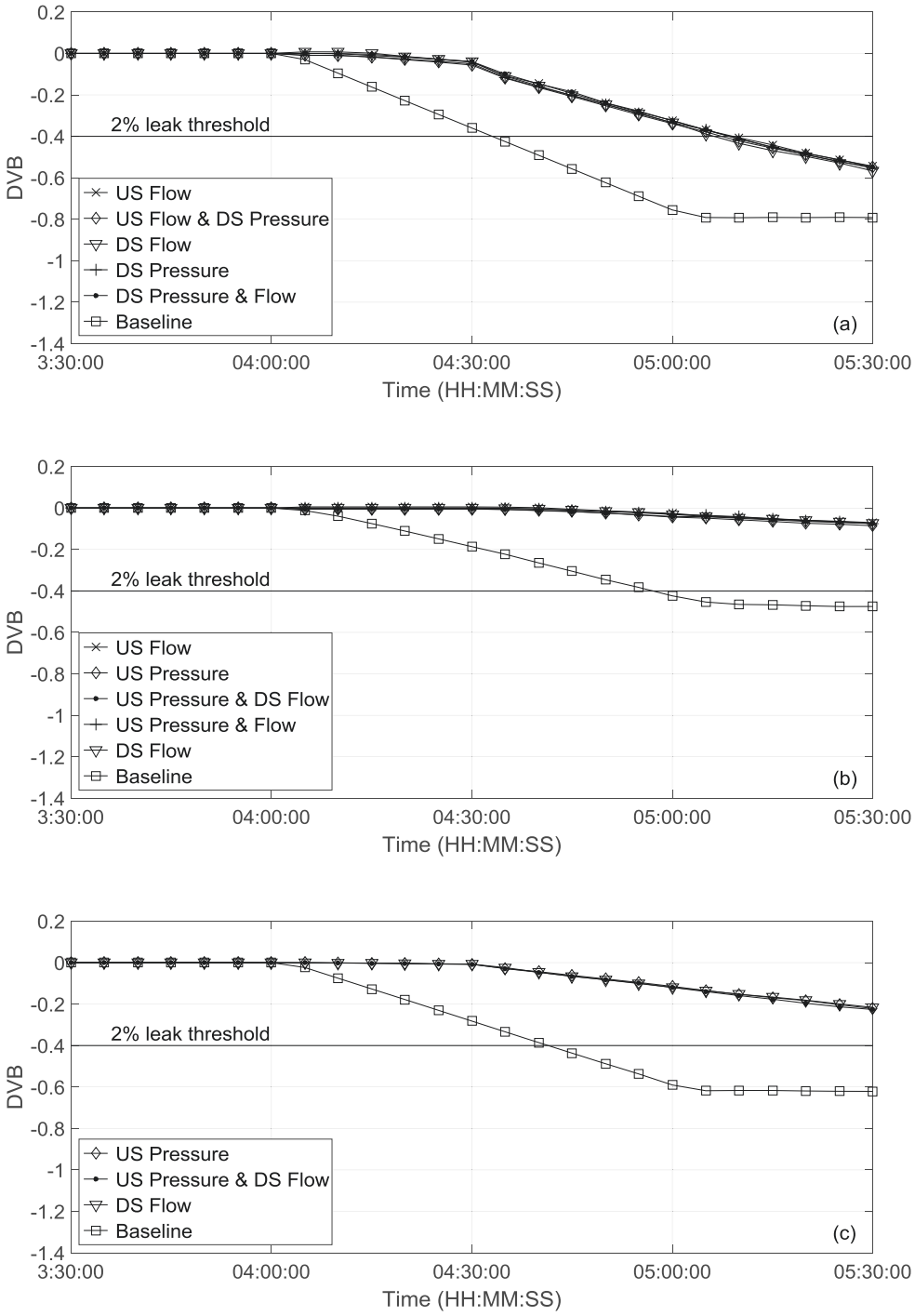

Figure 3-11. Effect of time skew on leak detectability in system of R = 2.20 with 1% random noise (sensors contain 10 seconds time skew): a) flow decrease; b) flow increase; c) steady state.

3.1.3 Uncertainty in Polling Time

Polling time of 5 seconds, and 10 seconds were tested in this study to see whether the loss of important measured data information during transient period would degrade leak detectability. Polling time of 1 second during transient period was considered as the baseline case for comparison. It was found that longer polling time in SCADA system had no effect on leak detectability, for either transient conditions or steady state. Since the *DVB* curves for the cases with longer polling time overlapped exactly onto the baseline for both perfect data and noisy data tests, the figures are not shown here.

3.1.4 Low *R* System vs High *R* System

The effect of uncertainties on leak detectability in systems with low and high *R* values was compared as they have distinctly different hydraulic responses. Computed leak detection times are summarized in Table 3-2 and 3-3 for perfect data and noisy data tests respectively along with the corresponding viscosity error, bulk modulus error, and time skew for each case. The change in detection times relative to the corresponding baseline case are also tabulated and negative numbers indicate earlier detection times compared to the baseline case. However, these were associated with excessive diagnostic flow caused by uncorrected errors rather than a leak. Figures of the *DVB* curves in the low *R* system for all tested scenarios can be found in Appendix A.

Note that setting *VER* to the same value in the two systems results in a significantly smaller *FPDC* bound in the low *R* system as the portion of the bound that is amplified by *VER* is proportional to flow rate. The correction that can be made to viscosity error in the low *R* system is greatly limited compared to the high *R* system.

Therefore, *VER* was set to different values in the low and high *R* systems to obtain the same *FPDC* bound in order to make a fair comparison. *VER* was set to its maximum value of 100% in the system with $R = 0.49$ which produced an *FPDC* bound ranging from 0.153 to 0.162 depending on the flow rate after transient. This bound range was equivalent to *VER* of 2 – 14% in the system with $R = 2.20$.

For the perfect data tests in Table 3-2, there was no clear indication on whether leak detectability was better in the high *R* or low *R* system. However, uncertainties had only minor impact on leak detectability when the "measured" data contained no noise. Thus, it was not important to determine the fine distinctions observed between the low *R* and high *R* systems. For noisy data tests however, the change in detection time from the baseline was smaller in the low *R* system as compared to the corresponding case in the high *R* system for 14 out of the 18 cases. For the remaining four cases, the two with time skew were undetected in both systems (i.e. *DVB* never crossed the threshold line); the other two cases with positive viscosity error had larger detection time change in the low *R* system but again the changes were very minor (within 1.5 minutes from the baseline). It can be concluded that in most cases, the system with low *R* value tends to be less impacted by uncertainties than the system with high *R* value.

Table 3-2. Change in detection time due to uncertainties in systems with low *R* and high *R* (perfect data tests).

Variable	Flow Condition	Level of Uncertainty	Baseline Detection Time		Change in Detection Time	
			R = 0.49	*R* = 2.20	*R* = 0.49	*R* = 2.20
Viscosity[1]	Flow Decrease	-20%*f*	24.2	24.9	0	0
		+20%*f*			0	0
	Flow Increase	-20%*f*	24.5	26.1	0	0
		+20%*f*			0	0
	Steady State	-20%*f*	24.4	25.5	0	0
		+20%*f*			0	0
Bulk Modulus	Flow Decrease	+10%	24.2	24.9	0.7	0
		-10%			1.7	4.9
	Flow Increase	+10%	24.5	26.1	0.5	0
		-10%			1.4	7
	Steady State	+10%	24.4	25.5	0.05	0.17
		-10%			-0.05	-0.2
Time Skew	Flow Decrease	10 s	24.2	24.9	2.5-3.9	0.6-3.1
	Flow Increase	10 s	24.5	26.1	0.8-2.2	0.5-3.3
	Steady State	10 s	24.4	25.5	0	0
Polling Time	Flow Decrease	5s, 10 s	24.2	24.9	0	0
	Flow Increase	5s, 10 s	24.5	26.1	0	0
	Steady State	5s, 10 s	24.4	25.5	0	0

[1]Viscosity error was introduced to obtain ±20% error in friction factor (*f*).

Table 3-3. Change in detection time due to uncertainties in systems with low *R* and high *R* (noisy data tests).

Variable	Flow Condition	Level of Uncertainty	Baseline Detection Time		Change in Detection Time	
			R = 0.49	*R* = 2.20	*R* = 0.49	*R* = 2.20
Viscosity[1]	Flow Decrease	-20%*f*	31.1	33.1	-1.8	-4.5
		+20%*f*			0.2	0.5
	Flow Increase	-20%*f*	55.5	61.7	-22.6	-34.2
		+20%*f*			1.3	0.1
	Steady State	-20%*f*	39.8	41.7	-8.7	-15.2
		+20%*f*			0.5	-0.3
Bulk Modulus	Flow Decrease	+10%	31.1	33.1	0.1	-1
		-10%			0.35	4.9
	Flow Increase	+10%	55.5	61.7	0	-4.6
		-10%			1.3	7.1
	Steady State	+10%	39.8	41.7	0.05	0.2
		-10%			-0.02	-0.3
Time Skew	Flow Decrease	10 s	31.1	33.1	28	35
	Flow Increase	10 s	55.5	61.7	Undetected	Undetected
	Steady State	10 s	39.8	41.7	Undetected	Undetected
Polling Time	Flow Decrease	5s, 10 s	31.1	33.1	0	0
	Flow Increase	5s, 10 s	55.5	61.7	0	0
	Steady State	5s, 10 s	39.8	41.7	0	0

[1]Viscosity error was introduced to obtain ±20% error in friction factor (*f*).

3.2 Random Error Sources

The *MCS* method was used to generate random values for viscosity, bulk modulus, time skew, polling time, and noise level. The purpose was to observe the probabilistic effect of uncertainties on leak detectability. Here the baseline was taken as the case without any error in viscosity or bulk modulus, 1-second polling time, no time skew, and with 1% random noise. It was found that the presence of random uncertainties caused the detection of a leak to be delayed or the leak to become undetectable in all cases.

The histogram in Figure 3-12 shows the percentage of delay in detection time as compared to baseline for the 500 cases experiencing flow decrease transient, for the low *R* and high *R* system, respectively. Leak was detected 31.1 minutes after the leak started for the low *R* system and 33.1 minutes for the high *R* system in the baseline cases. For the high *R* system, the mean value of the percentage delay was 46.5%, with a standard deviation of 24.8% and the median was 40.8%. For the low *R* system, the mean value was 31.8%, with a standard deviation of 17.2% and the median was 27.3%. This supports the previous finding that leak detection was generally less affected by uncertainties in the low *R* systems. It is interesting to see that the distribution for the high *R* system is clearly bimodal with peaks at approximately 25% and 65% in Figure 3-12b. The data centered around the peaks at 25% and 65% are associated with the cases with 1% and 2% random noise, respectively. Clearly the higher the noise level in the "measured" data, the more leak detectability is impacted by uncertainties. This was less clear in the low *R* system, but a bimodal distribution still exists with peaks at approximately 15% and 55%. There are very few data points past 60-70%, again supporting that it tolerates uncertainties better than the high *R* system.

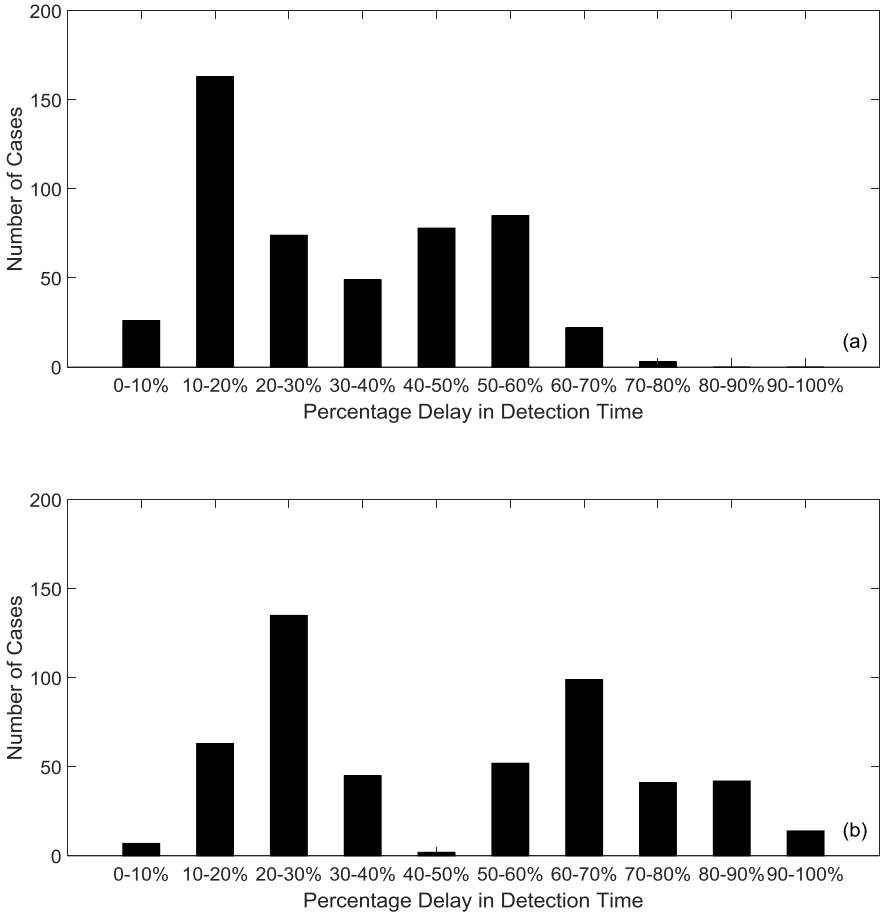

Figure 3-12. Delayed leak detection for the 500 cases with random uncertainties during flow decrease in system of: a) $R = 0.49$; b) $R = 2.20$.

Figure 3-13 presents the delay in detection time as a function of viscosity error and bulk modulus error respectively. Each data point represents one case and the two "layers" of data points are for cases with 1% data noise (lower layer) and 2% data noise (upper layer) respectively. This is corresponding to the bimodal distribution in Figure 3-12. It can be seen from the trend line that the delay does not have any trend with the magnitude of viscosity error (Figure 3-13a) but shows an obvious decreasing trend with bulk modulus error (Figure 3-13b). For tests with positive bulk modulus error the leak alarms were generated much closer to the baseline detection time as compared to

negative bulk modulus error cases. This was because scenarios with negative bulk modulus error required negative *BMC* but *BMC* was always positive for all the 500 cases since the transient event caused pressure to increase. This is consistent with the finding when single error source was present. Therefore an accurate measurement of bulk modulus is more important to leak detection than accurate viscosity. Only results from the high *R* system are shown as the trend is not obvious in the low *R* system.

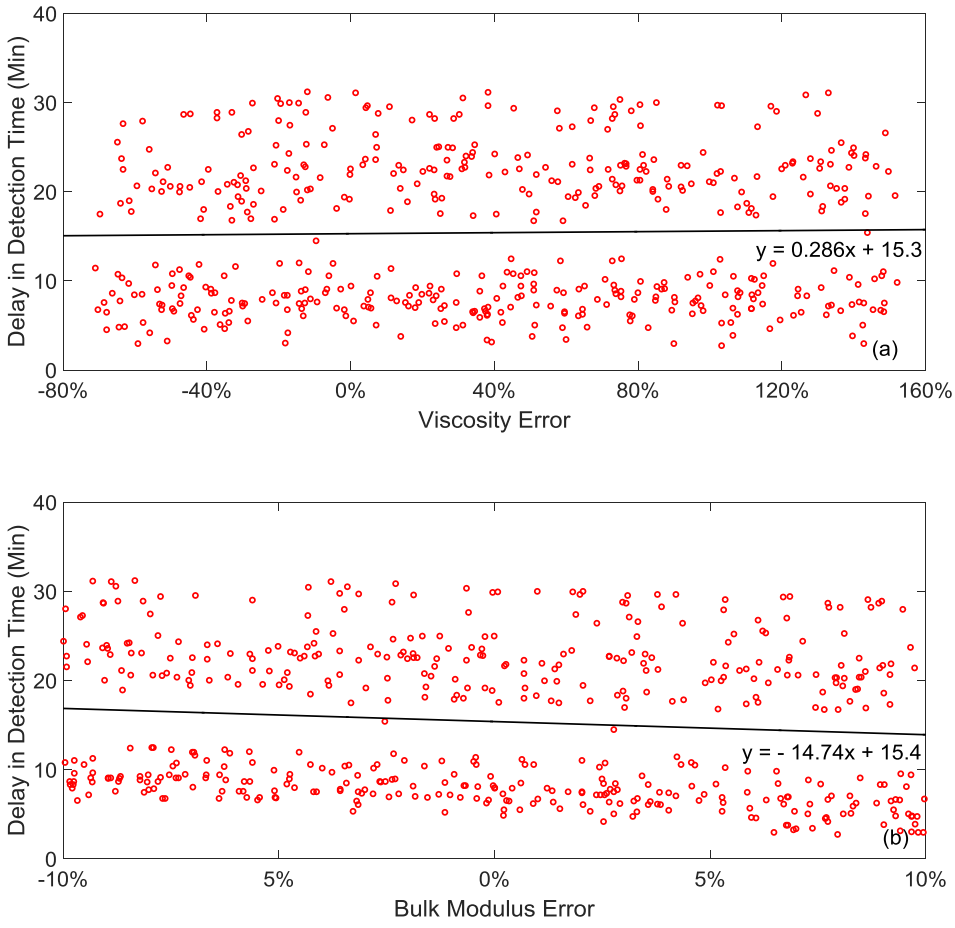

Figure 3-13. Delay in detection time as a function of a) viscosity error; b) bulk modulus error in system of $R = 2.20$ under flow decrease condition (black line is a linear fit to the data).

Figure 3-14 shows the delayed leak detection time with respect to time skew and polling time during flow decrease. The data points appear to be in two layers with the lower layer associated with 1% data noise and the top associated with 2% data noise. It can be seen from Figure 3-14a that in general tests with 10-second time skew experienced longer detection time than those with 5-second time skew. It was because the *EREP* was larger for cases with larger time skew (due to larger *TEB*). The discrepancy between the modelled and "measured" data was more attributed to measurement error than leak, resulting in degraded leak detectability. It is also interesting to notice that the degradation in leak detectability with the larger time skew is greater for 2% noise than 1% noise cases. This again can be explained from the *EREP* equation (2-10). Larger noise level leads to larger *FILP*, thus larger *EREP* and less *DF* (or *DVB*). The effect of polling time is shown in Figure 3-14b. Results were compared between 5-second and 10-second polling time for the different time skew value separately. It can be seen that tests with 5-second polling time were delayed to a larger extent for both 5-second and 10-second time skew scenarios. This could be explained with the *FILP* in equation (2-10). The slope of two measured points is much steeper for the tests with 5-second polling time than those with 10-second- polling time, so that *FILP* in 5-second polling time cases was generally steeper and resulted in larger *EREP*. Thus the leak was more difficult to detect with 5-second polling time.

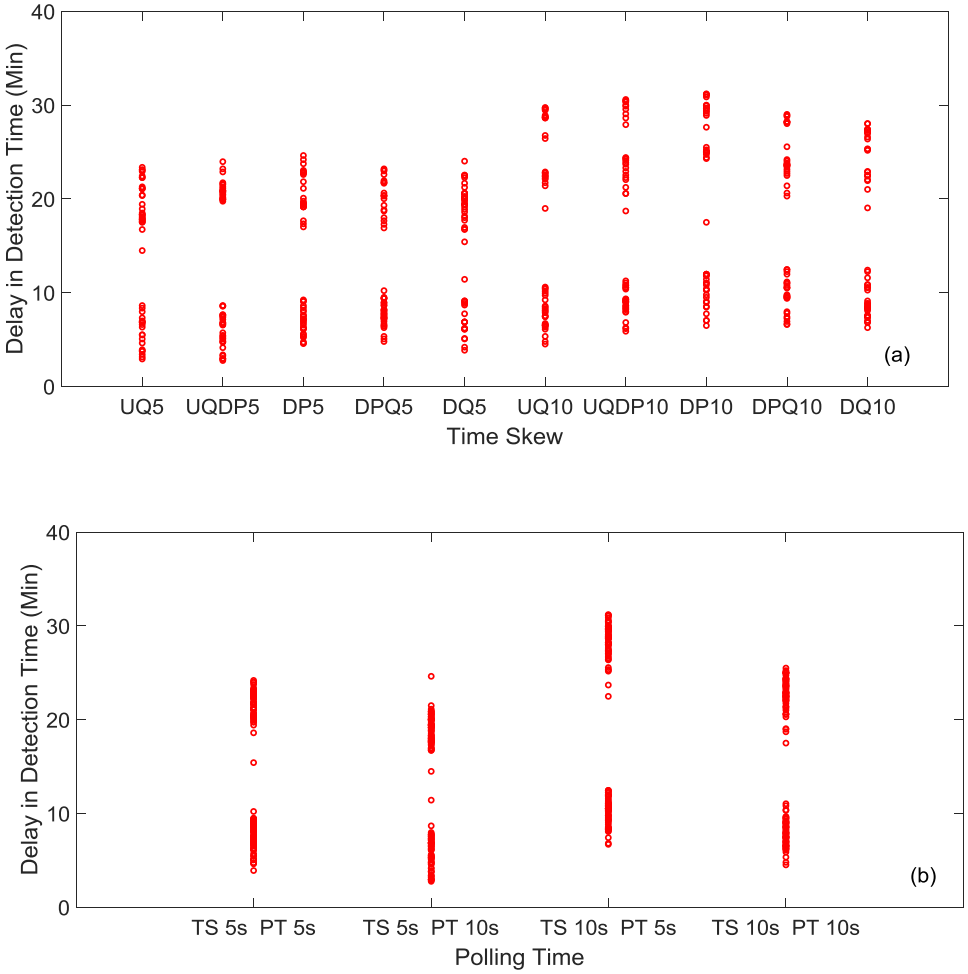

Figure 3-14. Delay in detection time as a function of a) time skew (TS); b) polling time (PT) in system of $R = 2.20$ during flow decrease.

The 5% leak became undetectable with the selected 2% leak threshold in a large number of scenarios during steady state and all 500 cases during flow increase. To better reveal the effects of random uncertainties, the leak alarm threshold was reduced to 1% leak for flow increase and steady state. Figure 3-15 shows the percentage of delay in detection time for the 500 cases experiencing a flow increase transient. For the baseline, the leak was detected 27.5 minutes and 31.9 minutes after it started in the low R and the high R system respectively. Even with the reduced threshold, there were still 215

undetectable cases in the low *R* system and 253 undetectable cases in the high *R* system. For the detected cases, the mean value of the percentage delay was 56.3%, with a standard deviation of 27.7% and the median was 54.3% in the low *R* system; the mean value was 73.9%, with a standard deviation of 32.2% and the median was 71.6% in the high *R* system. The results supported that the low *R* system was less affected by uncertainties than the high *R* system. Figure 3-16 and Figure 3-17 represent the delayed detection time for all detectable tests in terms of viscosity, bulk modulus, time skew, and poling time uncertainty respectively in the system with $R = 2.20$. The conclusions made for flow decrease cases remain valid here.

Figure 3-18 to Figure 3-20 summarize the results for random errors effects during steady state. With the 1% leak threshold, all 500 cases were detectable in the low *R* system. The baseline detection time was 20.6 minutes after leak started. The mean value of the percentage delay was 81.3%, with a standard deviation of 74.2% and the median was 54.3%. In the high *R* system, 445 scenarios were detectable with the baseline detection time of 22 minutes. The mean value was 124%, with a standard deviation of 102.8% and the median was 66.6%. The findings were consistent with those for transient conditions expect that the delay in detection time did not show a decreasing trend with bulk modulus error. This was because bulk modulus uncertainty had limited impact on leak detectability during steady flow condition.

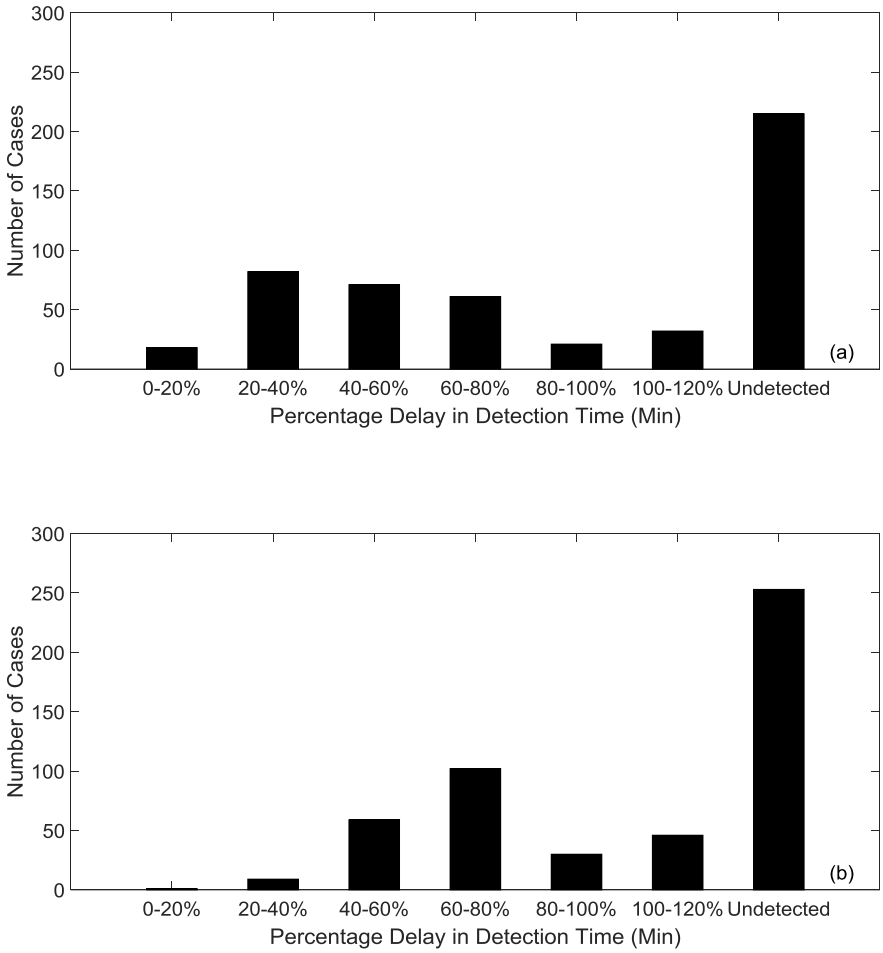

Figure 3-15. Delayed leak detection time for the 500 cases with random uncertainties during flow increase in system of: a) $R = 0.49$; b) $R = 2.20$.

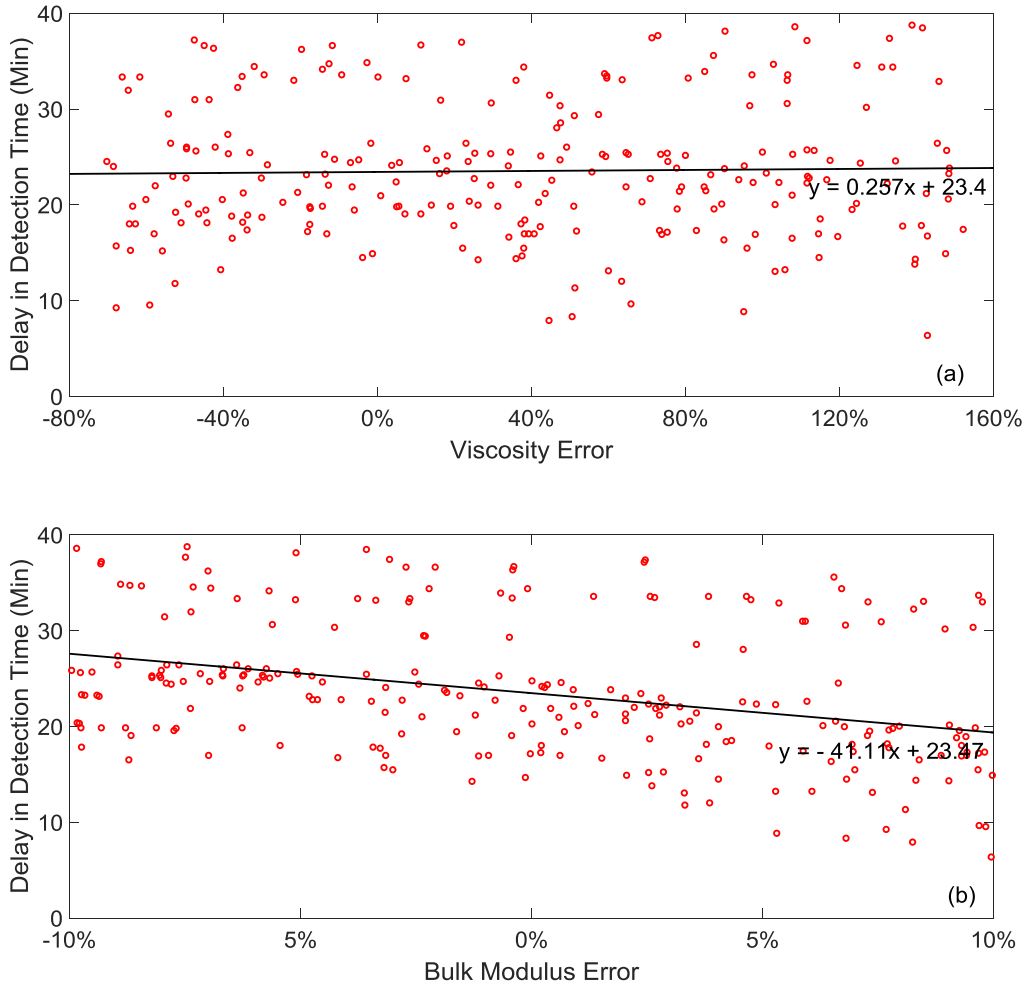

Figure 3-16. Delay in detection time as a function of a) viscosity error; b) bulk modulus error in system of R = 2.20 under flow increase condition (black line is a linear fit to the data).

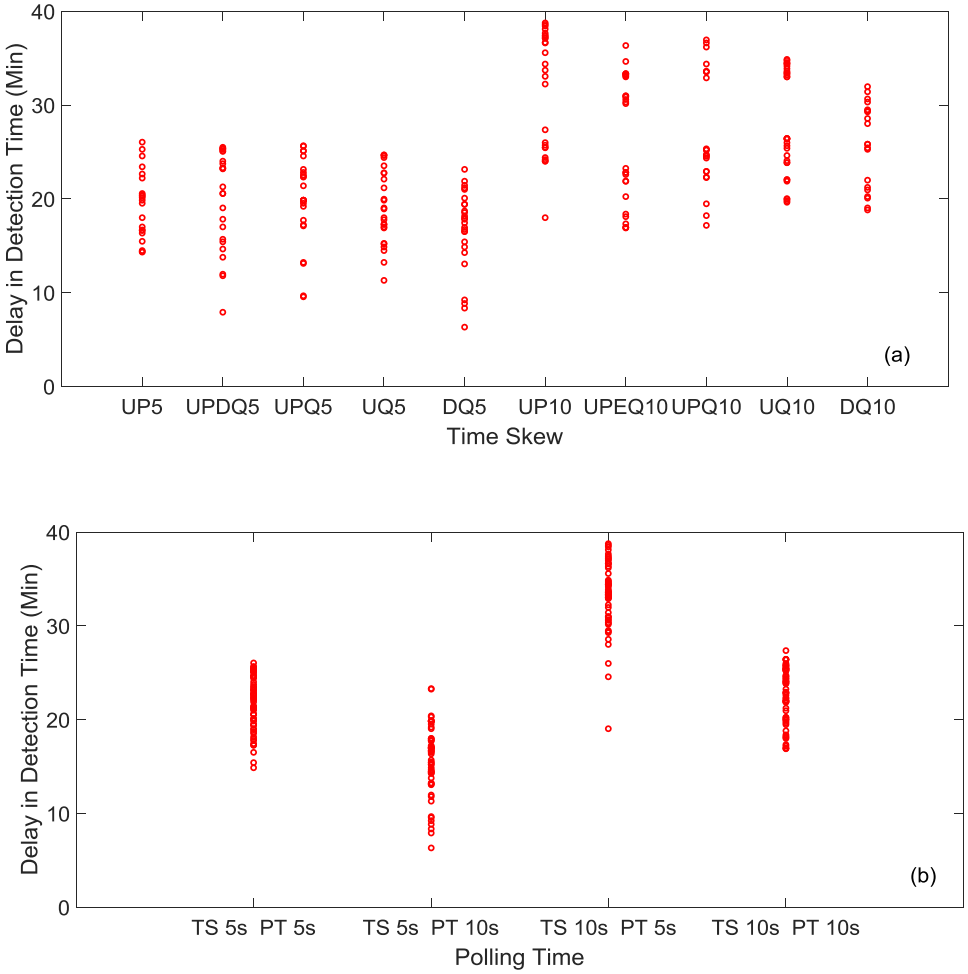

Figure 3-17. Delay in detection time as a function of a) time skew; b) polling time in system of R = 2.20 under flow increase condition.

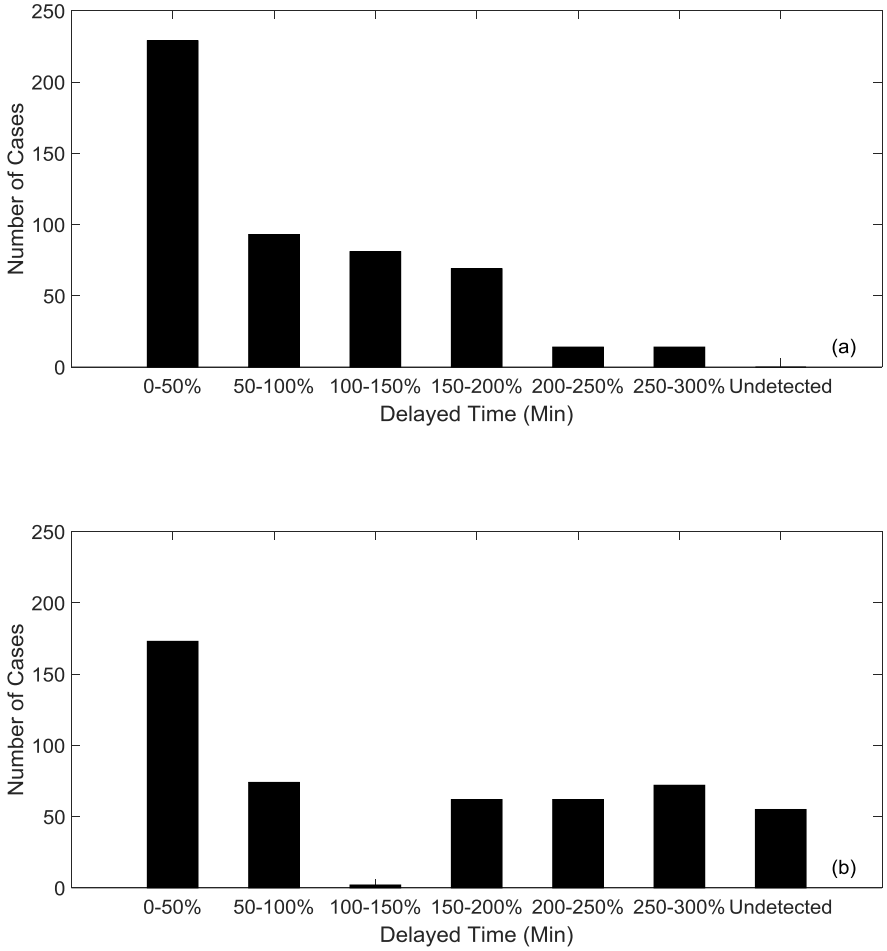

Figure 3-18. Delayed leak detection for the 500 cases with random uncertainties under steady flow condition in system of: a) $R = 0.49$; b) $R = 2.20$.

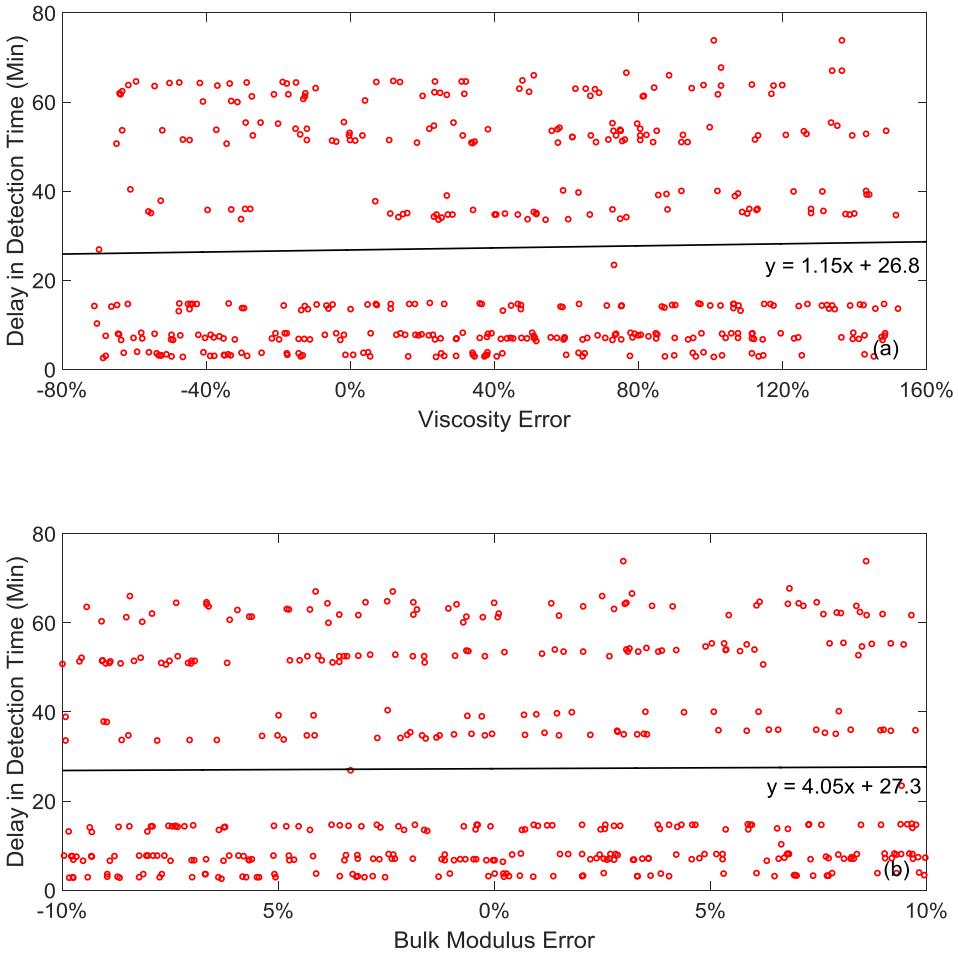

Figure 3-19. Delay in detection time as a function of a) viscosity error; b) bulk modulus error in system of $R = 2.20$ under steady flow condition (black line is a linear fit to the data).

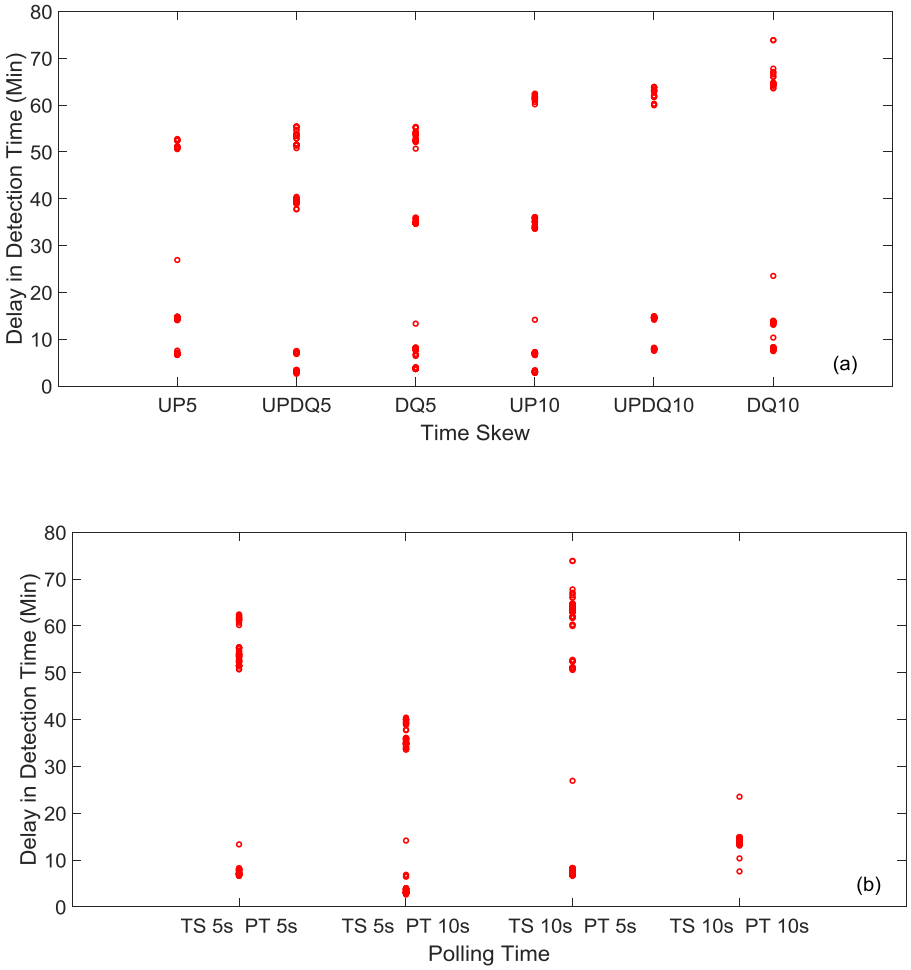

Figure 3-20. Delay in detection time as a function of a) time skew; b) polling time in system of $R = 2.20$ under steady flow condition.

Chapter 4: Summary and Conclusions

Computer model based leak detection systems use a hydraulic model to simulate the pipeline state and compare predictions to the hydraulic state indicated by field measurements. A discrepancy between the two states may be induced by a leak. However, real-world uncertainties can contribute towards discrepancies between the simulated and measured pipeline states even when a leak is not present. If a leak detection system cannot properly differentiate between the discrepancies caused by uncertainties and those caused by a leak, leak detectability is compromised and leaks may be missed or false alarms may be generated. This study investigated how various sources of uncertainty affect leak detection with the widely used *SPS Statefinder* leak detection software (DNV-GL 2012). Uncertainty sources investigated include fluid properties (viscosity and bulk modulus), SCADA parameters (polling time and time skew), and field sensors (data noise). Uncertainties were introduced into the leak detection system individually and collectively, and the changes in leak detection time compared to a baseline case with no uncertainties were determined for a simulated 5% leak. Both steady state and transient operating conditions were considered in this study.

It was found that the *SPS Statefinder* leak detection system can cope better with errors in viscosity than in bulk modulus. Leak detectability was unaffected by viscosity errors as long as *Statefinder* was configured to allow it to fully correct the friction factor. In the case of bulk modulus errors, full correction was only achievable when the bulk modulus correction coefficient was set equal to the exact amount of required correction and when the pressure wave propagated in a certain pattern. That is, when there is positive error in the bulk modulus and the transient causes the pressure to increase in the

pipeline; or there is negative error in bulk modulus and the transient causes pressure to decrease in the pipeline. Longer polling time alone did not affect leak detectability but time skew caused significant degradation of leak detectability during both steady and transient operating conditions when the "measured" data contained random noise. Therefore, a general ranking of the importance of the uncertainty sources (from high to low) is: (1) time skew as it always causes degraded leak detectability; (2) bulk modulus error as it may be incorrectly adjusted in some cases and the required amount of correction is often not known; (3) viscosity error as it only has impact when full correction is not allowed and the data is noisy; and (4) polling time as it alone does not affect leak detectability for the cases tested. The probabilistic effect of random uncertainties of all sources caused delayed leak detection in all cases. It was shown that systems with a low *R* factor were less sensitive to uncertainties compared to system with high *R* factor. The findings are applicable to a wide category of *real-time transient model*-based leak detection systems which utilize optimization algorithm to minimize the difference between the modelled and measured pipeline state.

This study provides general guidelines in terms of prioritizing enhancement measures for the tested or similar leak detection system. The implications of the findings are: accurate measurement of bulk modulus in real pipeline system is important (as compared to viscosity) because there are certain conditions for which bulk modulus error cannot be properly accounted for, resulting in degraded leak detectability. The software developer may be involved to review the algorithm used for adjusting wave speed to explore if it can possibly be improved so that correct adjustment can always be made to error in bulk modulus regardless of the pattern of wave propagation. The time skews with

SCADA data, if they can be reduced, will lead to more accurate state estimation and better leak detectability. The noise level in field sensors is also an important affecting factor for leak detection and it can greatly amplify the impact of other uncertainties that may exist in the system. A data filter could be employed or better sensors could be installed to reduce data noise. Pipeline systems of low *R* factor can generally better tolerate uncertainties or data noise. Measures can be taken to reduce *R* factor for existing pipelines, e.g. adding flow meters to reduce the length of the pipe segment. Variables comprising the *R* factor should be considered when designing new pipelines and their leak detection systems.

In this study, the only leak location tested was at the mid-point of the pipeline. This is because a previous study showed that leak detectability was not very sensitive to leak locations comparing leaks located at 1/4, 1/2, and 3/4 of the pipe length (Pabon, 2015). Future work is recommended for additional leak locations especially nearby field sensor locations. Only the worst transient conditions with single severity were used for the transient operating scenarios evaluated. Therefore, the effects of uncertainties on leak detectability should be evaluated with other transient scenarios with various severities to cover a full range of operating conditions. Other sources of uncertainty such as pipe elevation, shape and diameter, and temperature may also be added in future studies.

References

Al-Khomairi, A. (2008). Leak detection in long pipelines using the least squares method. *Journal of Hydraulic Research*, *46*(3), 392-401.

Al-Zahrani, M. (2014). Modeling and Simulation of Water Distribution System: A Case Study. *Arabian Journal for Science & Engineering (Springer Science & Business Media BV)*, *39*(3).

American Petroleum Institute (2002). API 1130: Computational pipeline monitoring for liquids. *American Petroleum Institute report*.

American Petroleum Institute (1993). API 1149: Pipeline variable uncertainties and their effects on leak detectability. *American Petroleum Institute report*.

American Petroleum Institute (2015). API 1149: Pipeline variable uncertainties and their effects on leak detectability, second edition. *American Petroleum Institute report*.

Canadian Energy Pipeline Association (2016). About pipelines: How are leaks detected in an underground pipeline? Available at: https://www.aboutpipelines.com/en/preventing-incidents/leak-detection/

Canadian Energy Pipeline Association (2016). Taking action on our commitment to Canadians. Available at: http://www.cepa.com/wp-content/uploads/2016/06/16-CEPA-0010_PerformanceReport_2016_EN_low.pdf

Canadian Standards Association (2007). Z662-07 Oil and gas pipeline systems: Annex E: Recommended practice for liquid hydrocarbon pipeline system leak detection, 388-392.

Central Intelligence Agency (2016). The World Factbook. Available at: https://www.cia.gov/library/publications/the-world-factbook/fields/2117.html

Covas, D., & Ramos, H. (2010). Case studies of leak detection and location in water pipe systems by inverse transient analysis. *Journal of Water Resources Planning and Management*, *136*(2), 248-257.

DNV-GL (2012). Stoner Pipeline Simulator (SPS) 9.9.0 *Help and Reference*.

Duan, H. F., Lee, P. J., Ghidaoui, M. S., & Tung, Y. K. (2011). Leak detection in complex series pipelines by using the system frequency response method. *Journal of hydraulic research*, *49*(2), 213-221.

Duan, H. F. (2015). Uncertainty analysis of transient flow modeling and transient-based leak detection in elastic water pipeline systems. *Water resources management*, *29*(14), 5413-5427.

Geiger, G. (2006) State-of-the-Art in Leak Detection and Localisation. *1st Pipeline Technology 2006 Conference*, April 2006, Hannover, Germany.

National Energy Board (NEB) (2016) Safety Performance Portal. Available at: https://www.neb-one.gc.ca/sftnvrnmnt/sft/dshbrd/index-eng.html

Pabon, S. (2015). Sensitivity study of a computer model based leak detection system in liquid pipelines (Master dissertation, *University of Alberta*).

Rossman, L. A. (2002). Epanet User's Manual, Environmental Protection Agency, EPA, Cincinnati.

United States Department of Transportation (2007). Leak Detection Technology Study, *For PIPES Act*, H.R.5782.

Vinh, P. (2012). Adding value to CPM testing, in: *2012 American Petroleum Institute Pipeline Conference and Cybernetics Symposium*.

Wylie, E. B., Streeter, V. L., & Suo, L. (1993). Fluid transients in systems. Englewood Cliffs, NJ: Prentice Hall.

Appendix A: Tests for 5% leak in a system of $R = 0.49$.

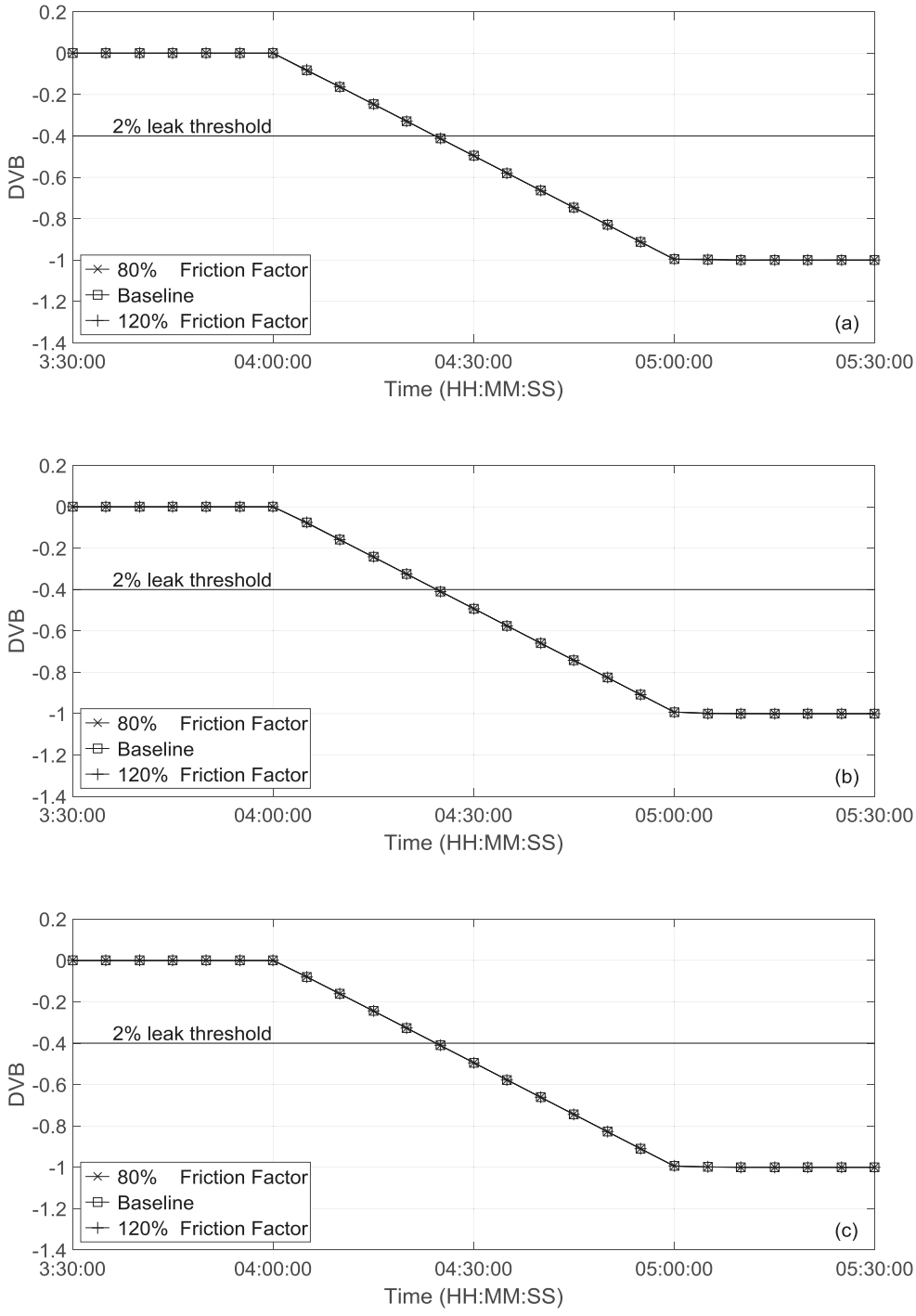

Figure A.1. Effect of viscosity error on leak detectability in system of $R = 0.49$ with perfect data: a) flow decrease; b) flow increase; c) steady state.

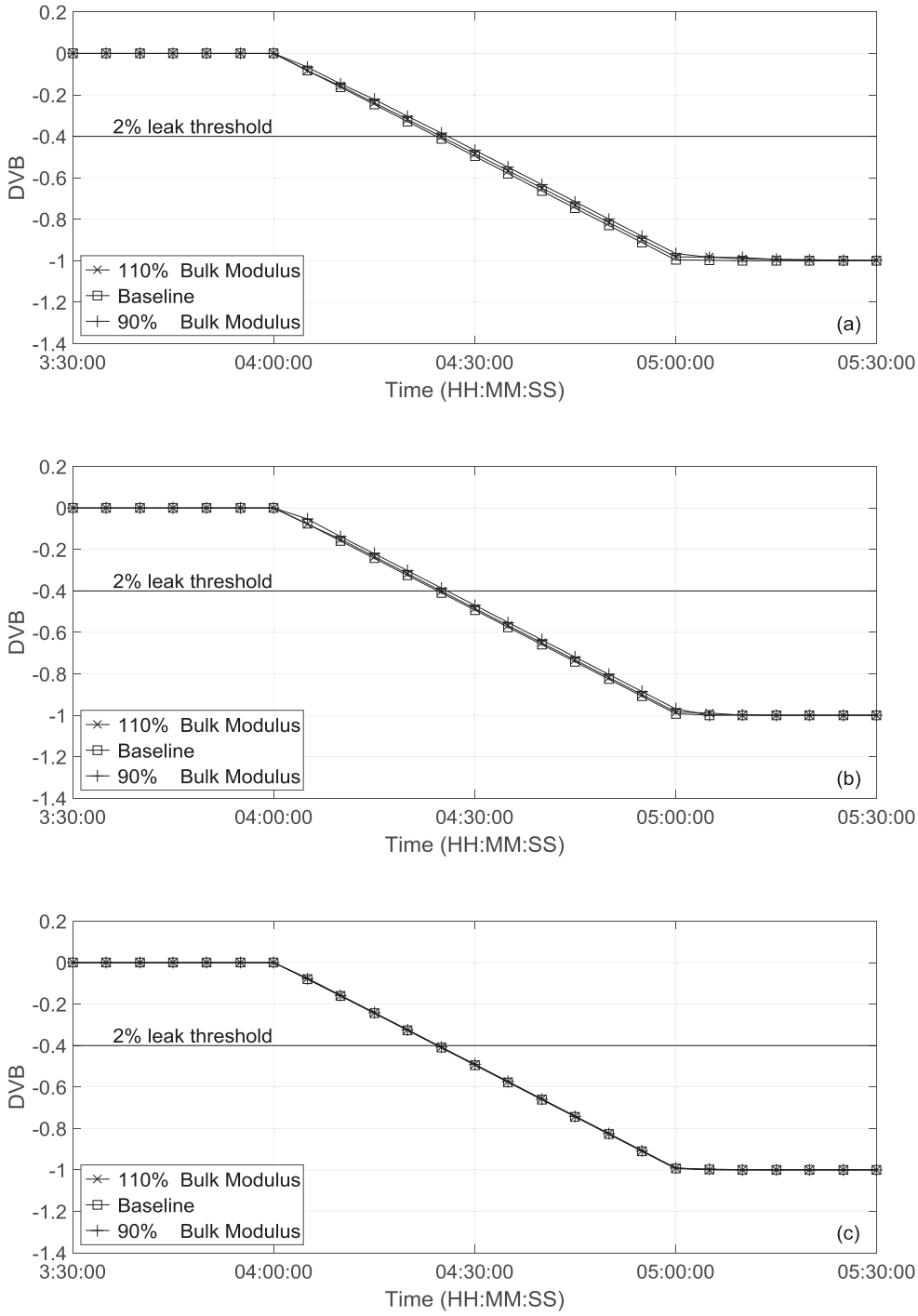

Figure A.2. Effect of bulk modulus error on leak detectability in system of $R = 0.49$ with perfect data: a) flow decrease; b) flow increase; c) steady state.

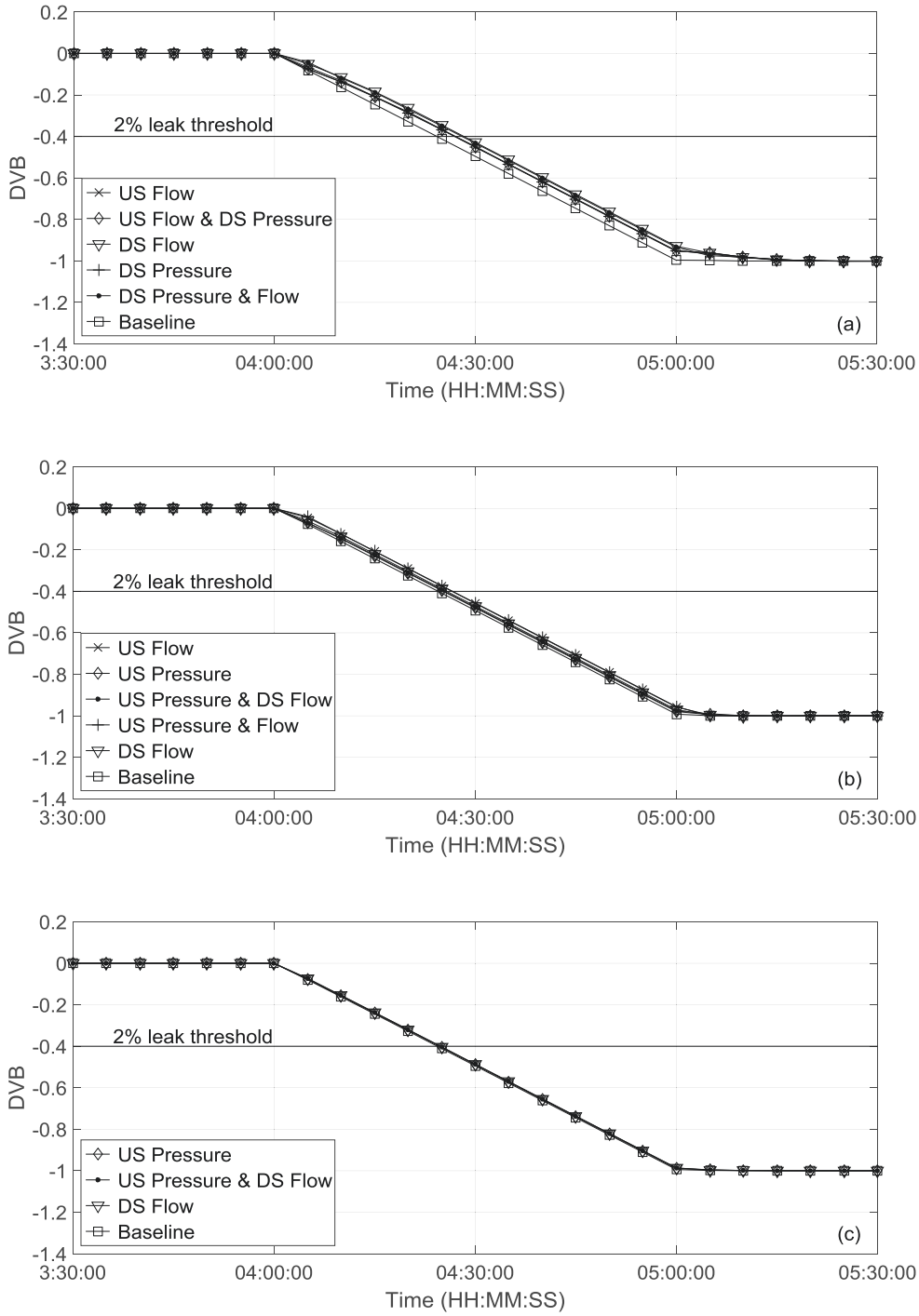

Figure A.3. Effect of time skew on leak detectability in system of $R = 0.49$ with perfect data: a) flow decrease; b) flow increase; c) steady state.

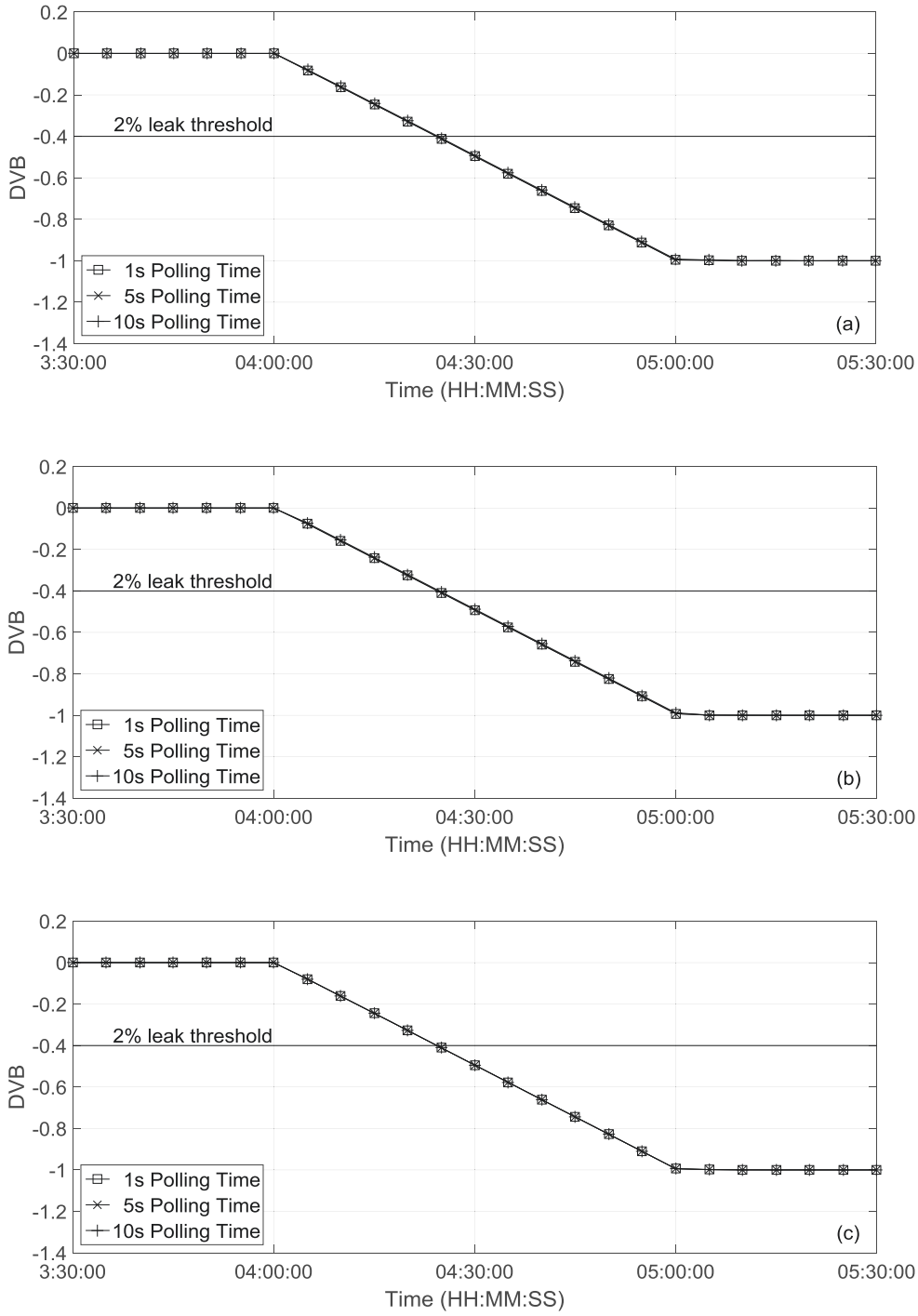

Figure A.4. Effect of longer polling time on leak detectability in system of $R = 0.49$ with perfect data: a) flow decrease; b) flow increase; c) steady state.

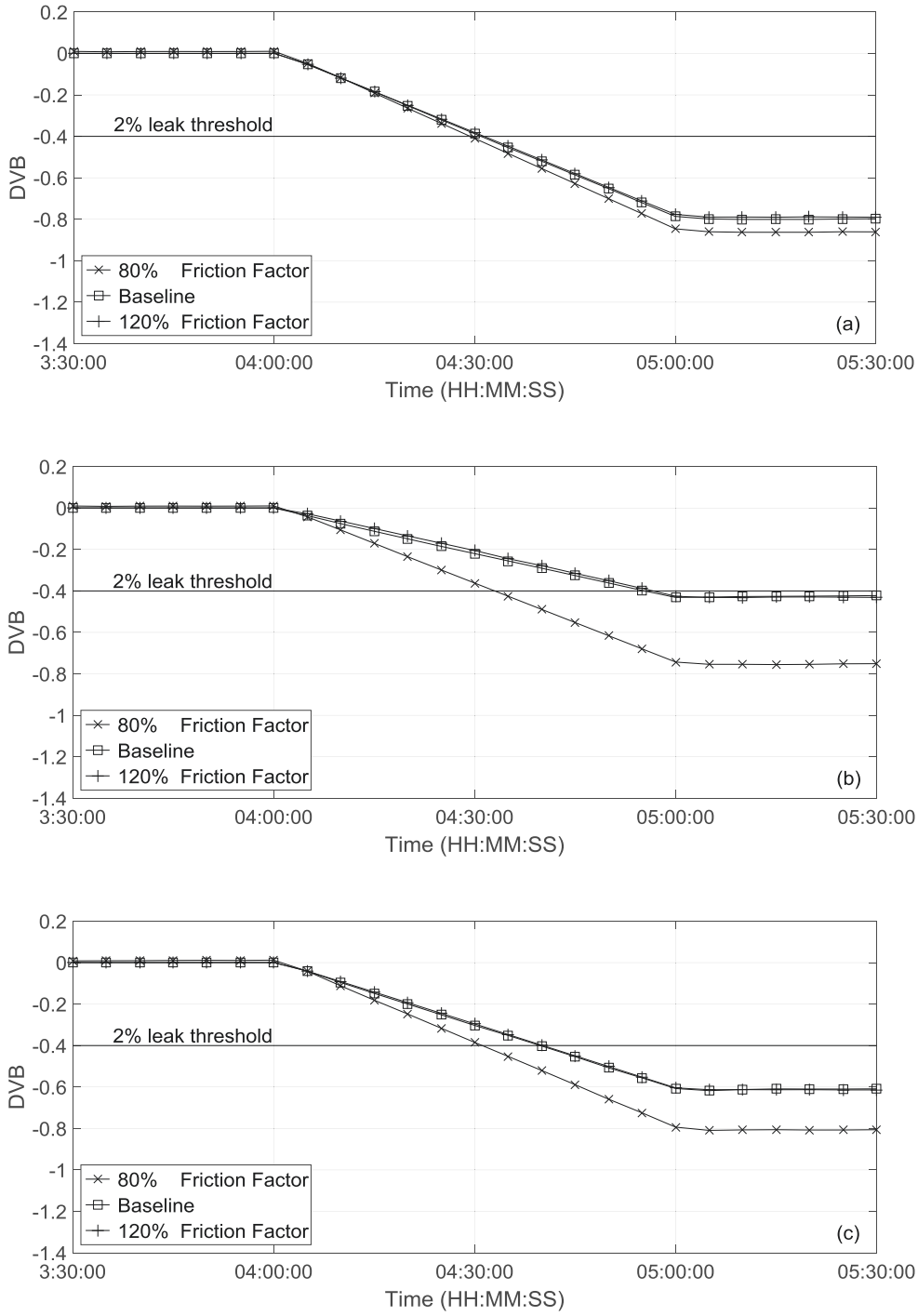

Figure A.5. Effect of viscosity error on leak detectability in system of $R = 0.49$ with 1% random noise: a) flow decrease; b) flow increase; c) steady state.

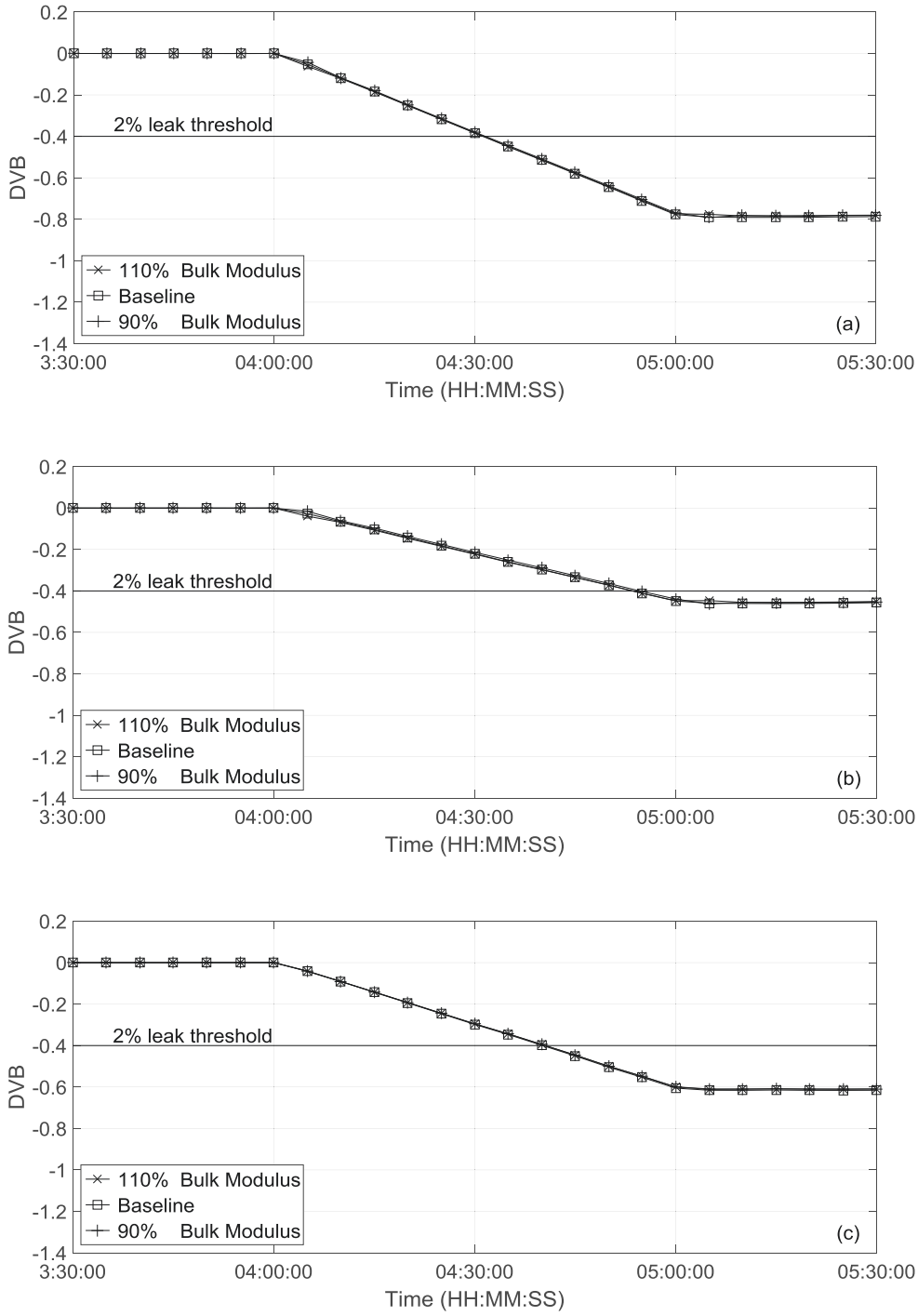

Figure A.6. Effect of bulk modulus error on leak detectability in system of $R = 0.49$ with 1% random noise: a) flow decrease; b) flow increase; c) steady state.

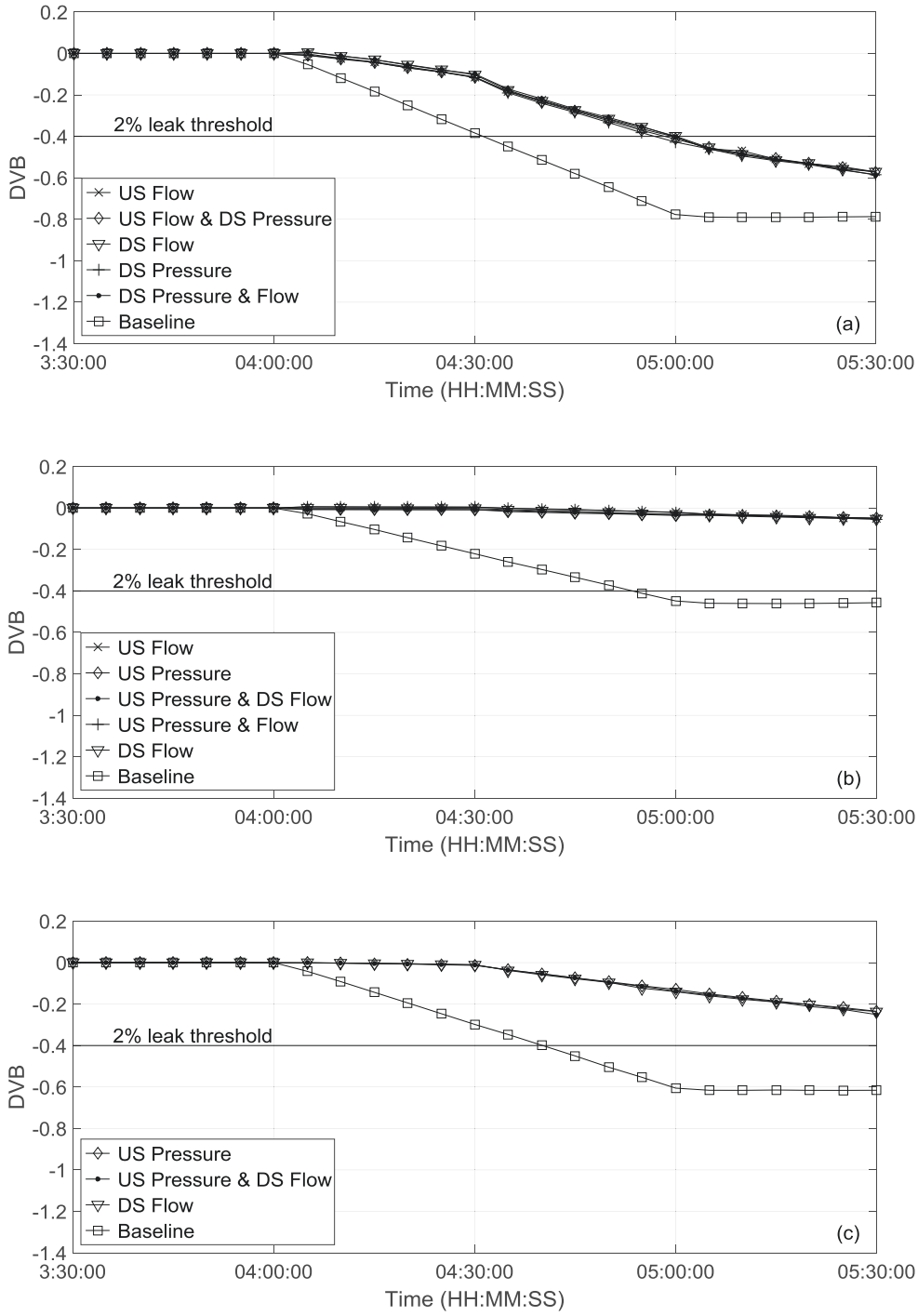

Figure A.7. Effect of time skew on leak detectability in system of $R = 0.49$ with 1% random noise: a) flow decrease; b) flow increase; c) steady state.

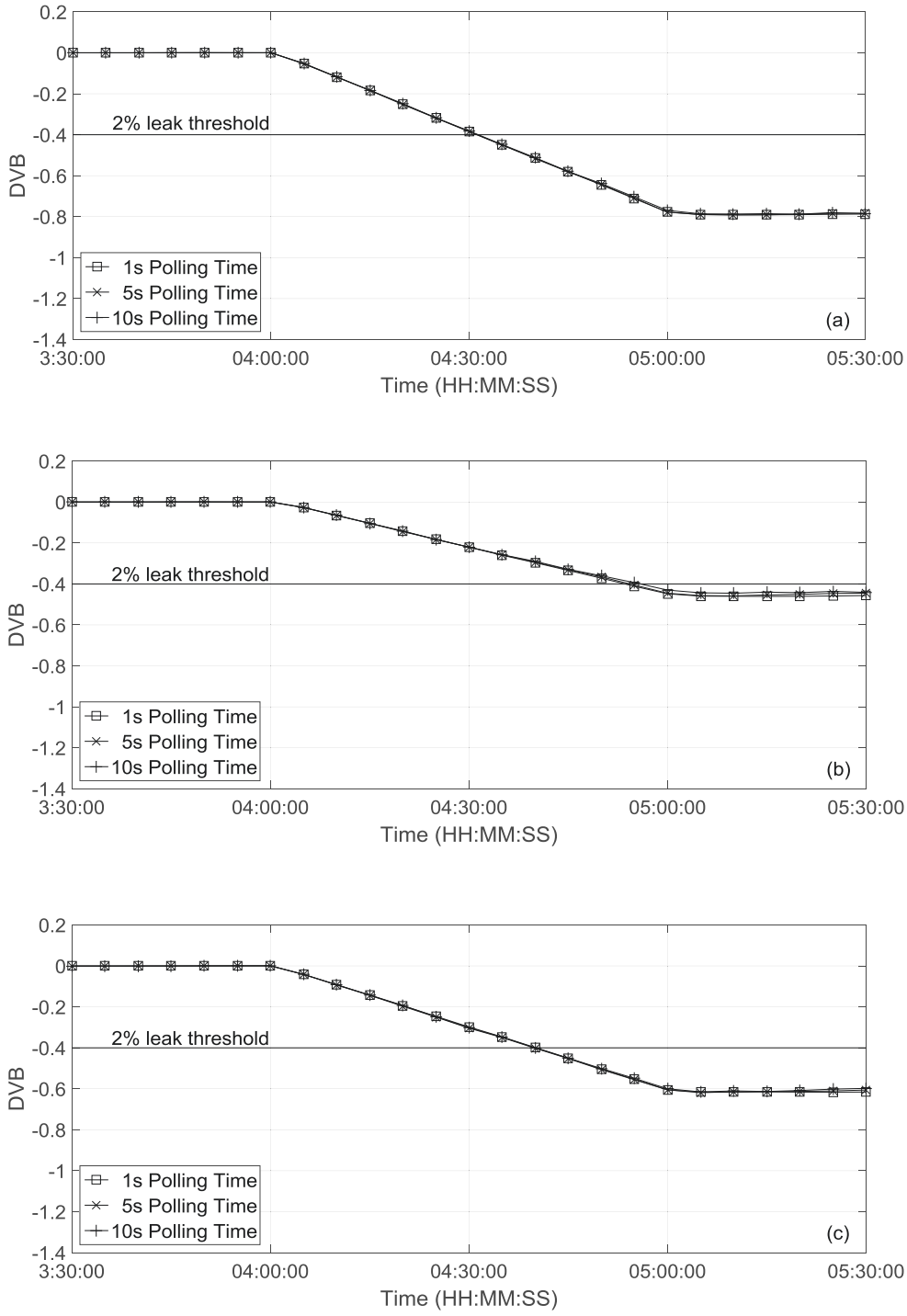

Figure A.8. Effect of longer polling time on leak detectability in system of $R = 0.49$ with 1% random noise: a) flow decrease; b) flow increase; c) steady state.

Appendix B: Tests for 2% leak with 1% random noise.

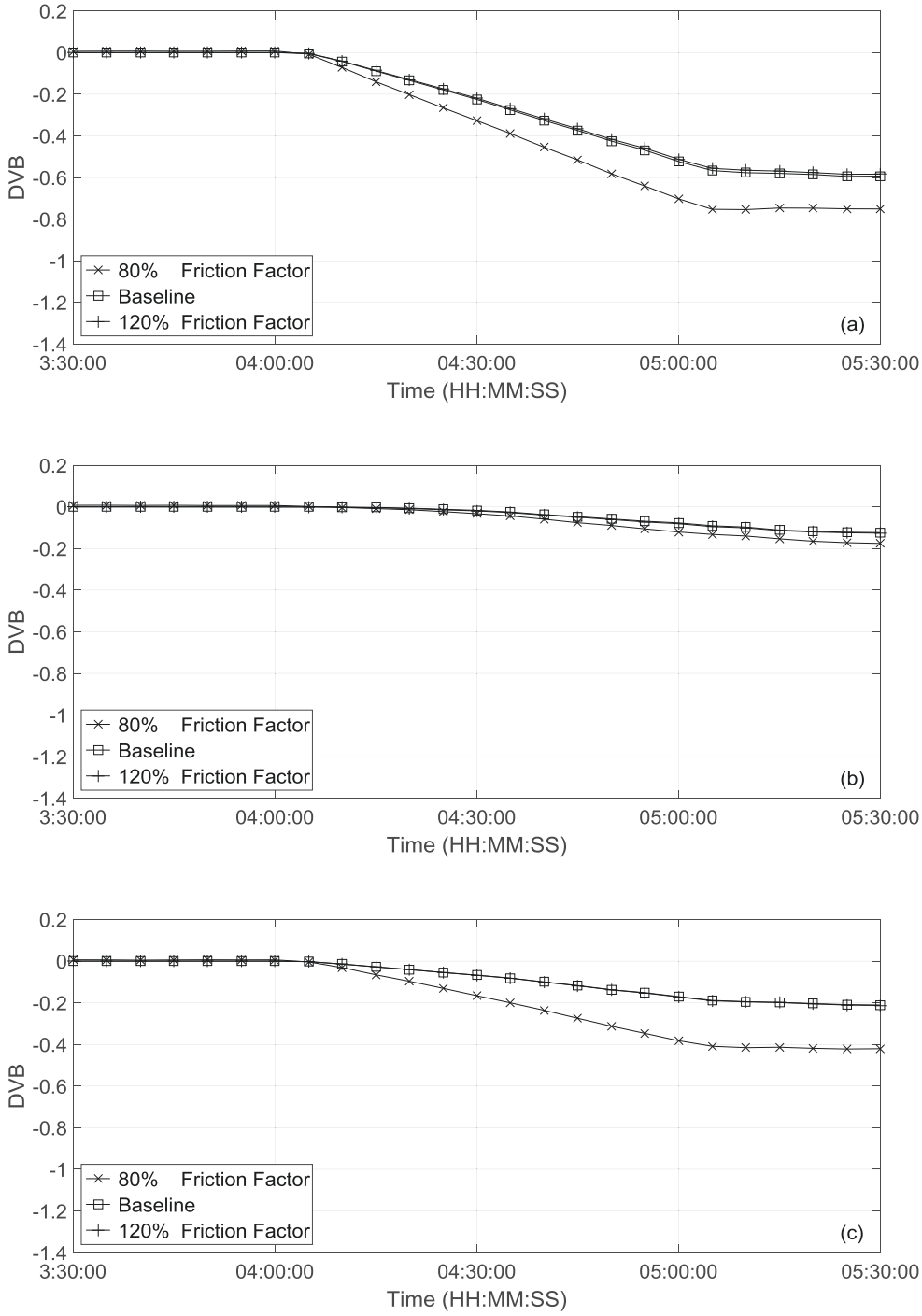

Figure B.1. Effect of viscosity error on leak detectability in system of $R = 2.20$: a) flow decrease; b) flow increase; c) steady state.

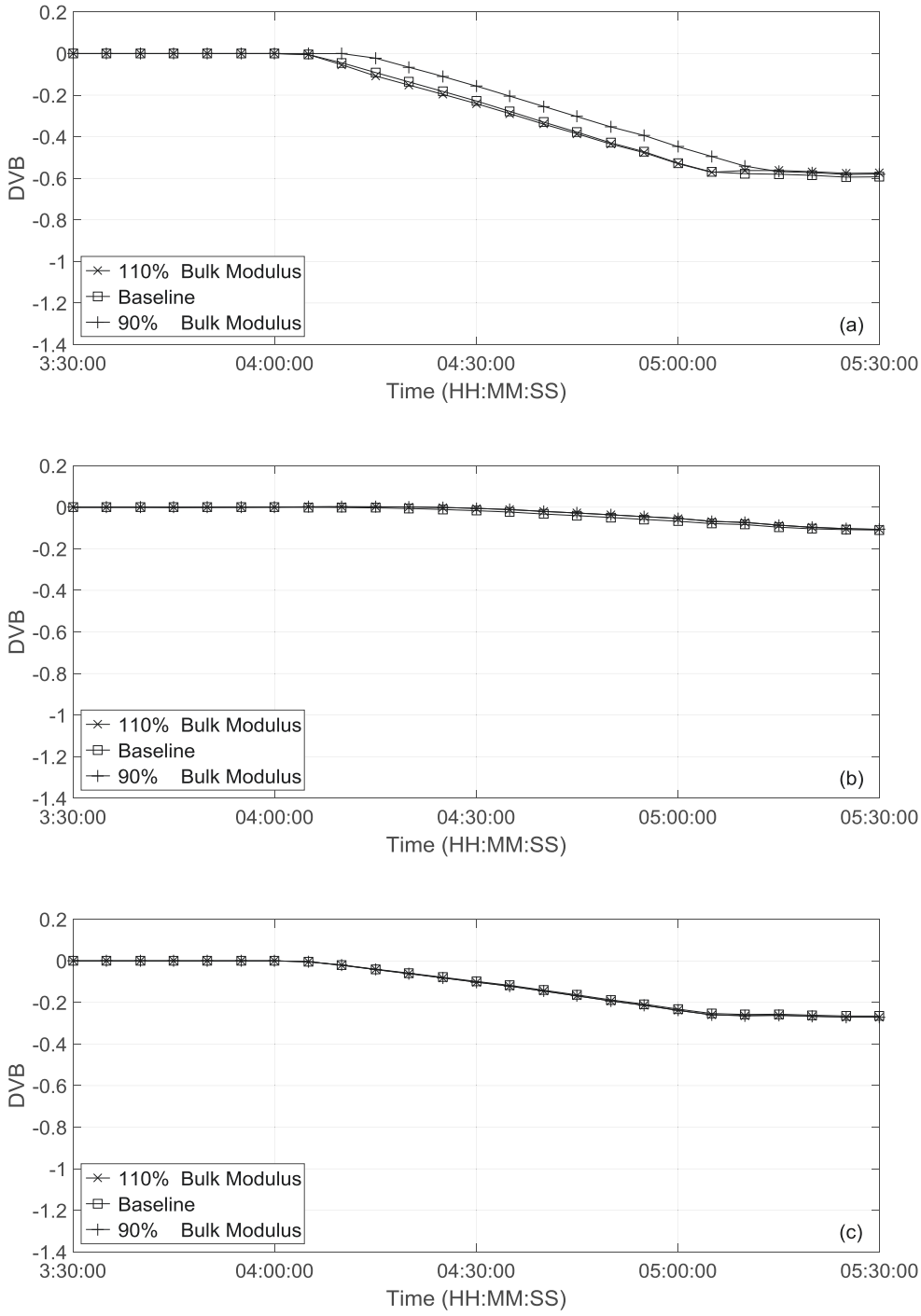

Figure B.2. Effect of bulk modulus error on leak detectability in system of R = 2.20: a) flow decrease; b) flow increase; c) steady state.

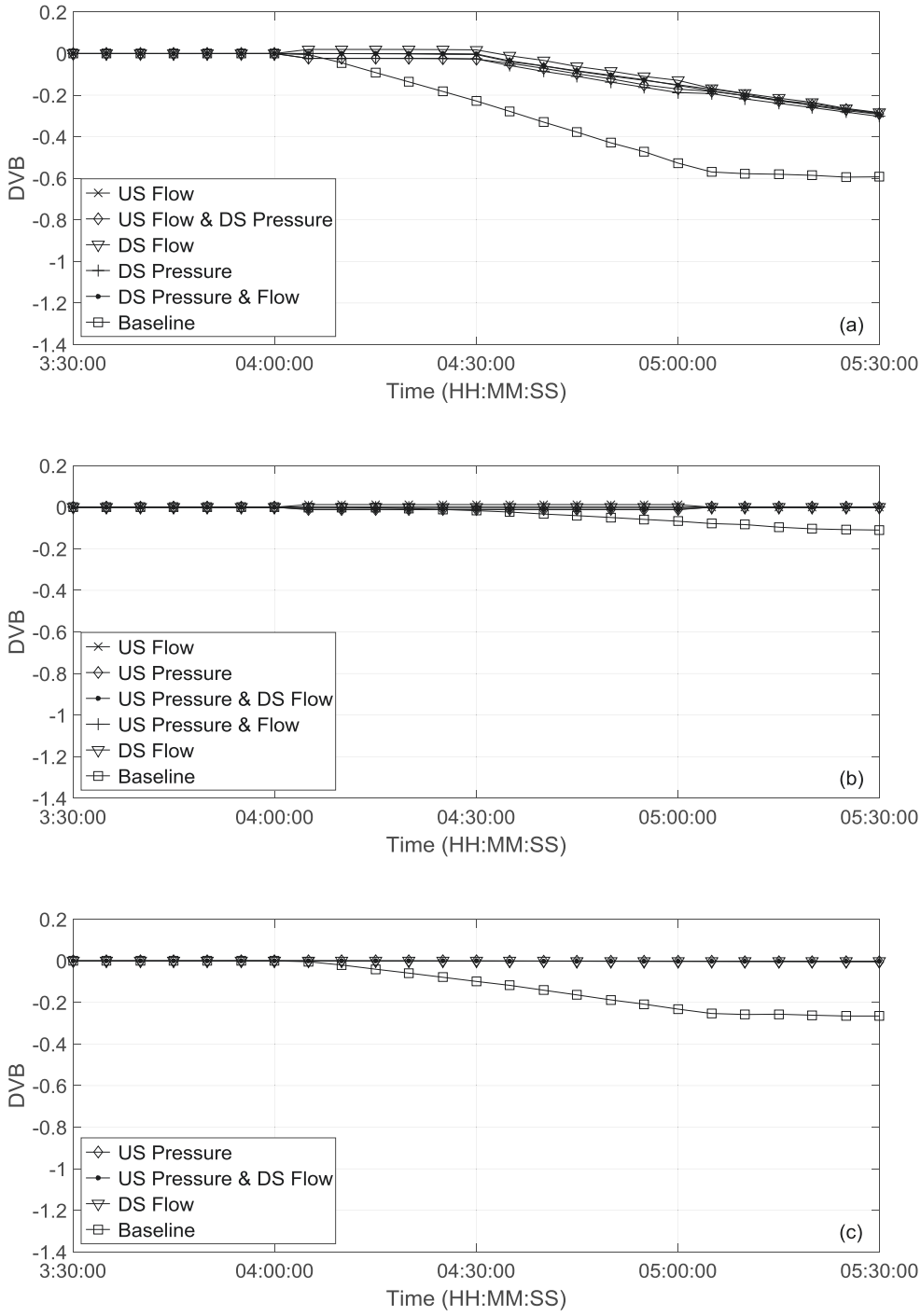

Figure B.3. Effect of time skew on leak detectability in system of $R = 2.20$: a) flow decrease; b) flow increase; c) steady state.

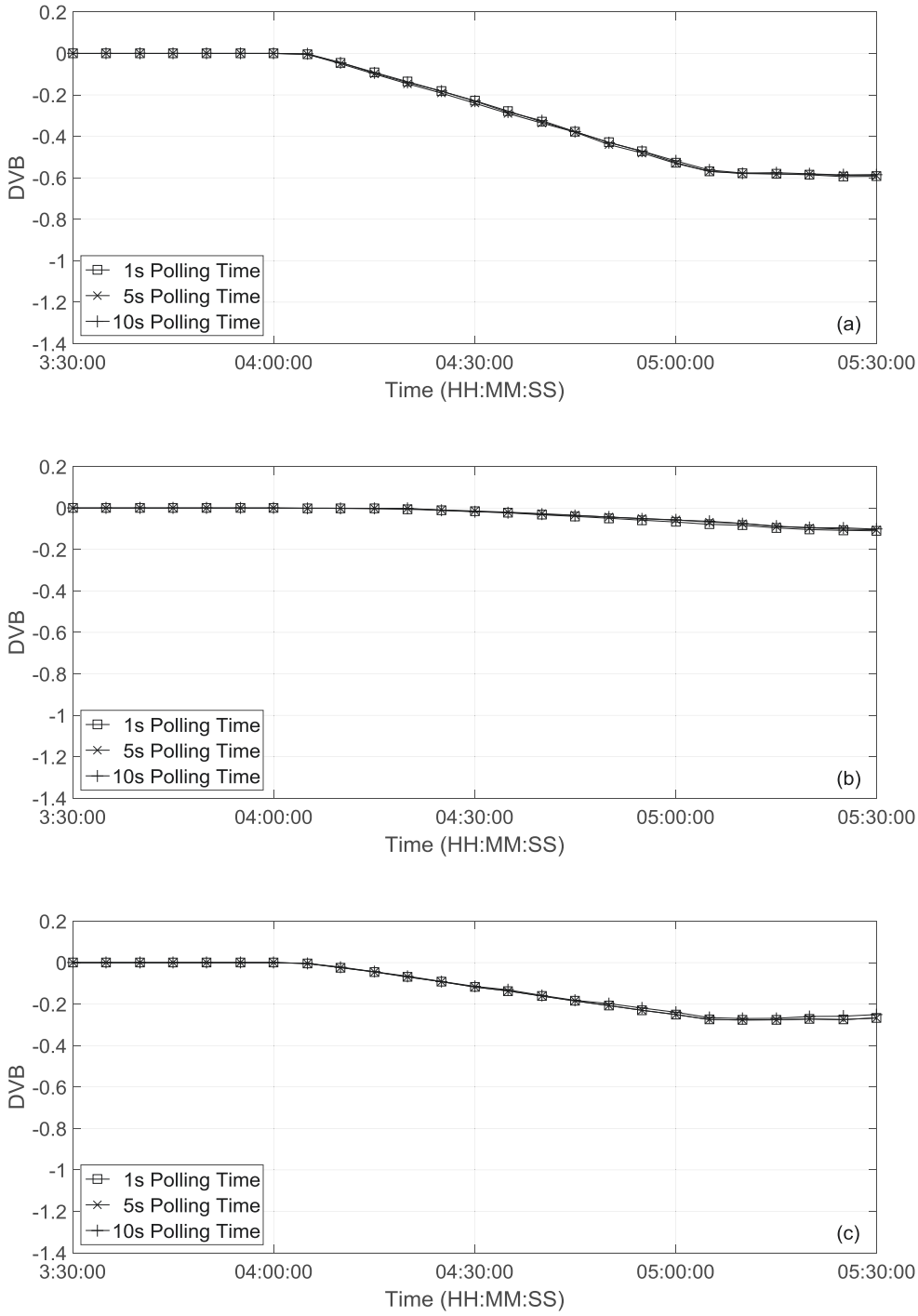

Figure B.4. Effect of longer polling time on leak detectability in system of $R = 2.20$: a) flow decrease; b) flow increase; c) steady state.

Appendix C: Tests for 30% leak with 1% random noise.

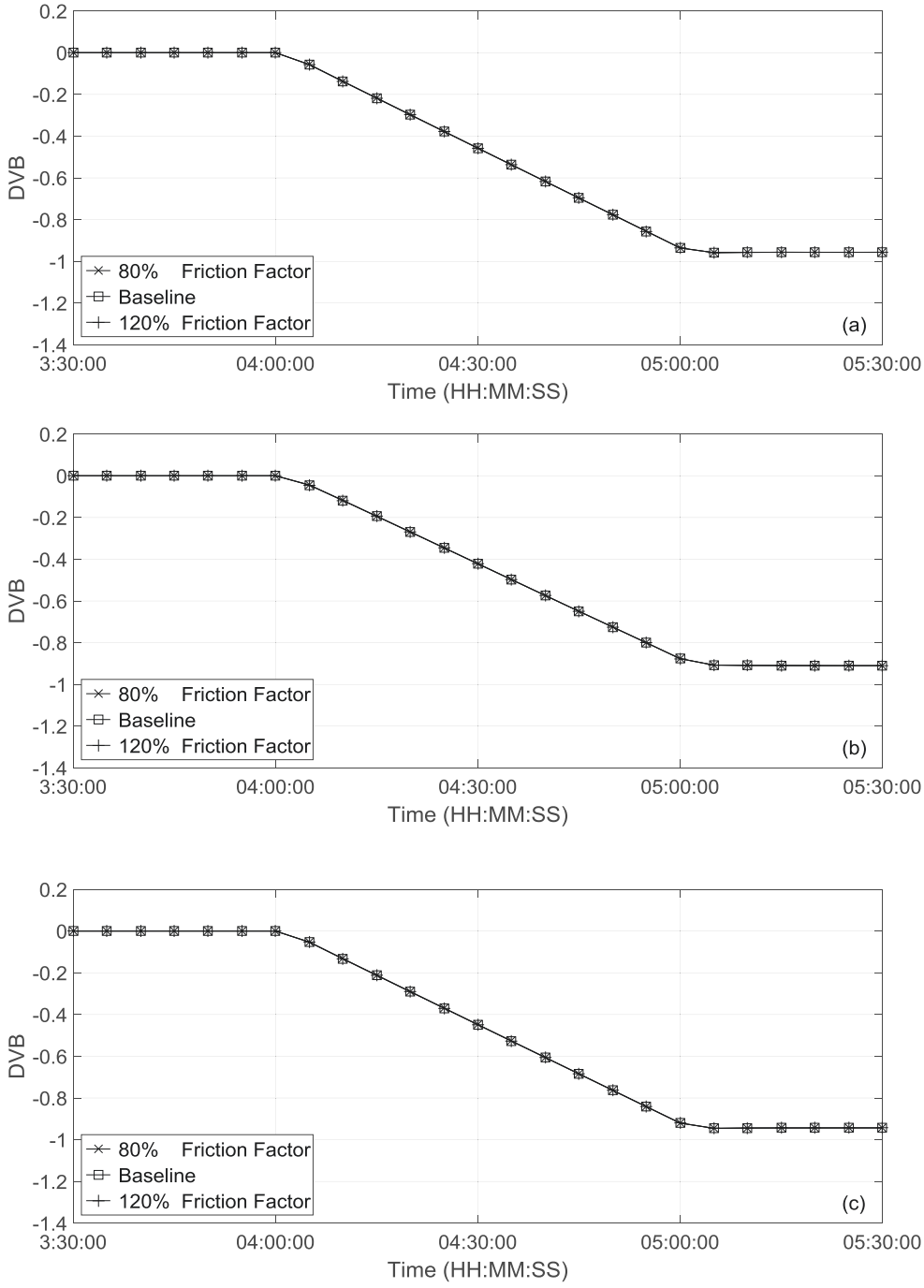

Figure C.1. Effect of viscosity error on leak detectability in system of $R = 2.20$: a) flow decrease; b) flow increase; c) steady state.

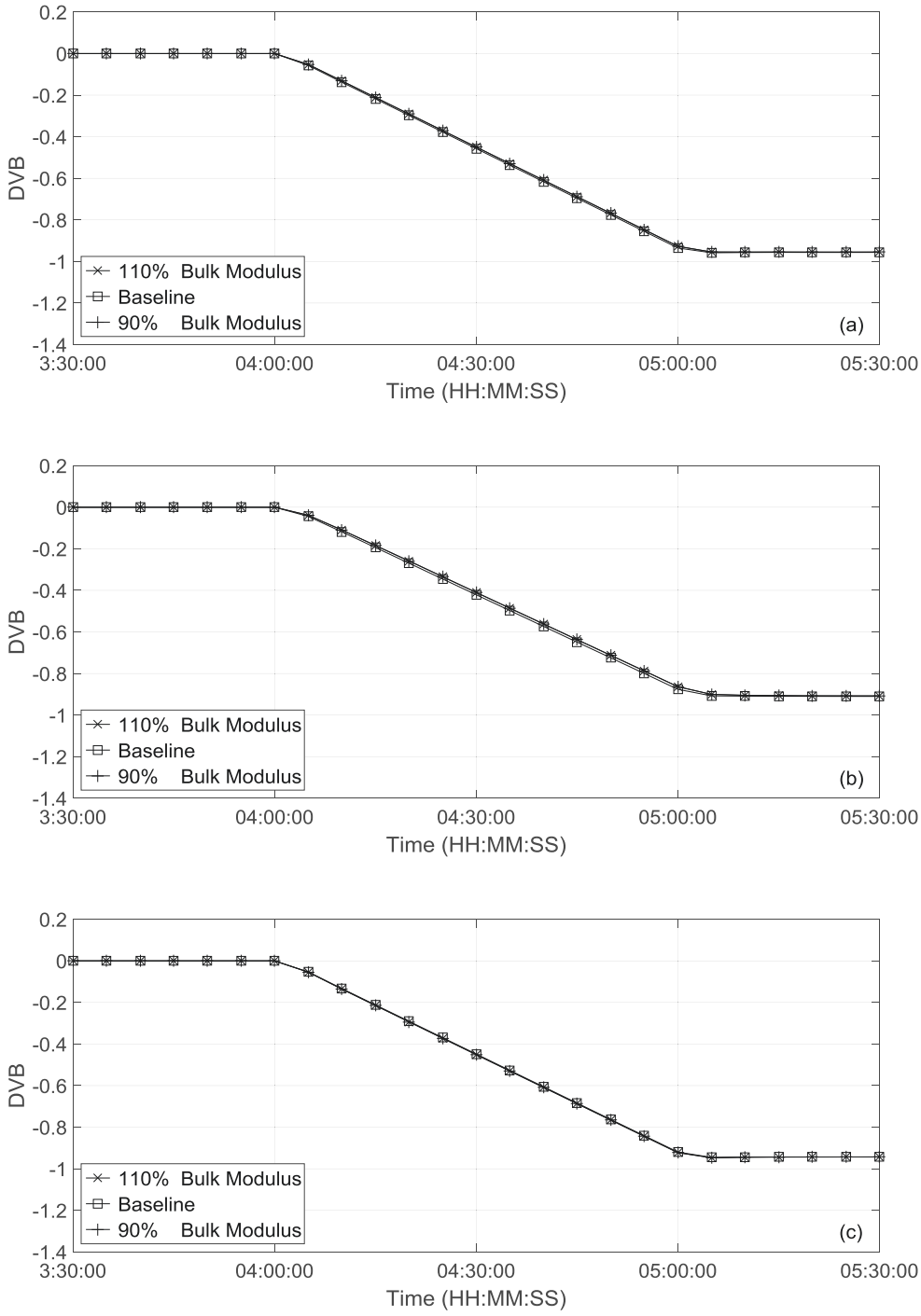

Figure C.2. Effect of bulk modulus error on leak detectability in system of R = 2.20: a) flow decrease; b) flow increase; c) steady state.

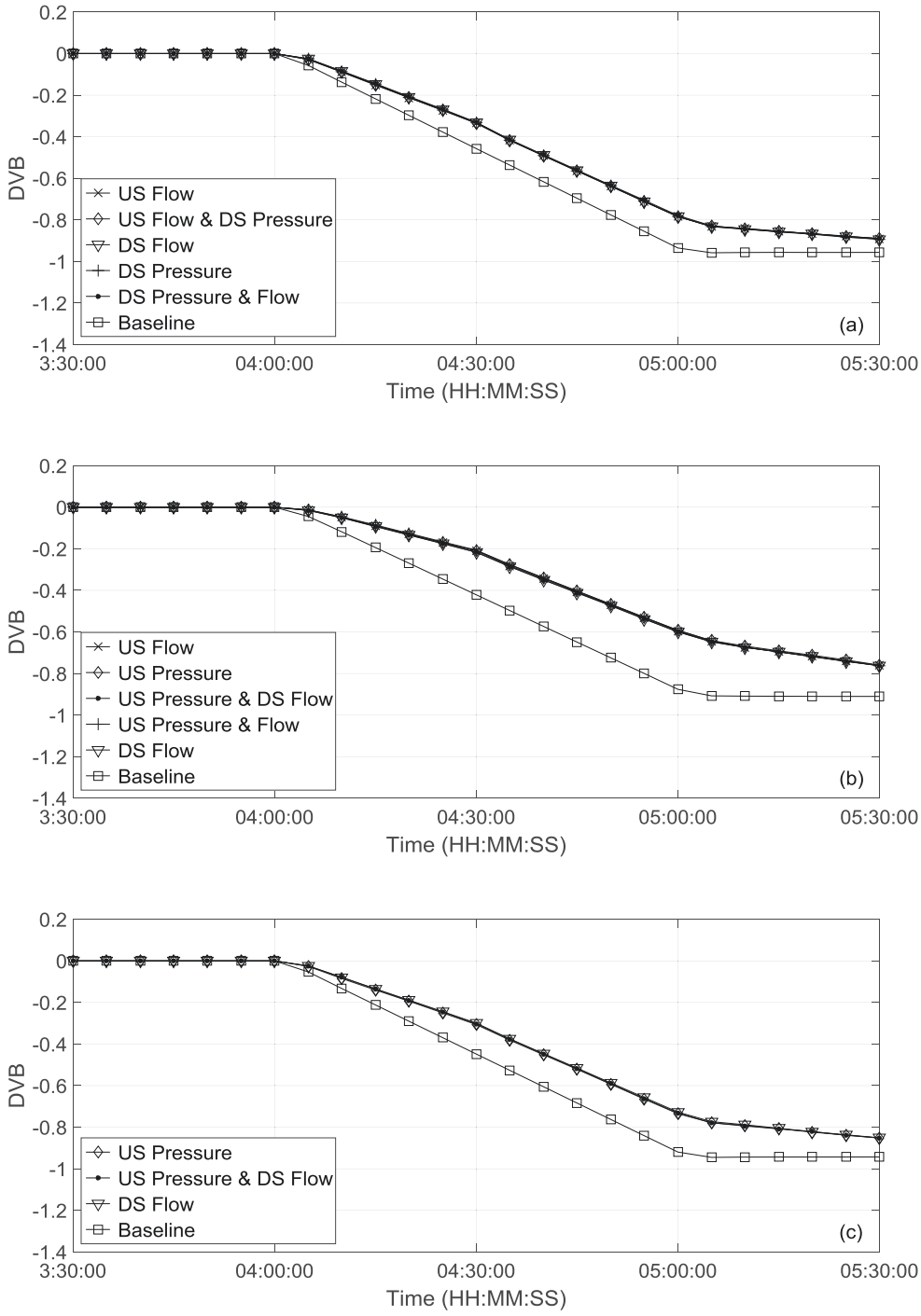

Figure C.3. Effect of time skew on leak detectability in system of $R = 2.20$: a) flow decrease; b) flow increase; c) steady state.

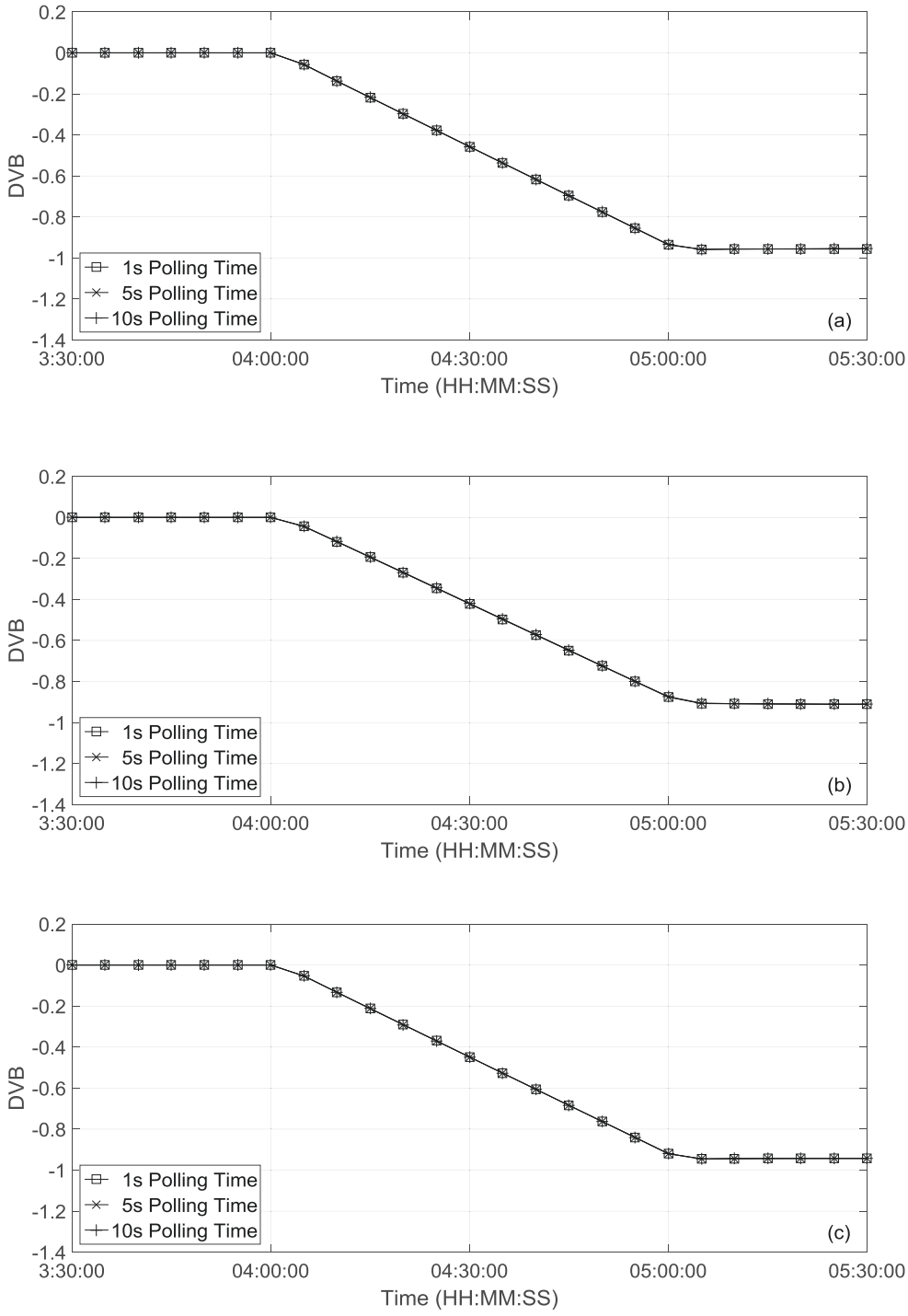

Figure C.4. Effect of longer polling time on leak detectability in system of $R = 2.20$: a) flow decrease; b) flow increase; c) steady state.